

## ABSTRACT

Title of Document:                    EXPRESSION AND DISTRIBUTION OF  
  BUTYROPHILIN 1A1 AND XANTHINE  
  DEHYDROGENASE-OXIDASE                 IN  
  LACTATING MAMMARY GLAND

Li Tao, Master of Science, 2006

Directed By:                            Professor, Ian. H. Mather, Departments of  
  Animal and Avian Sciences and Cell Biology  
  and Molecular Genetics

Milk-lipid droplets are secreted from mammary epithelial cells with an outer envelope of membrane, called the milk lipid globule membrane, which consists of a phospholipid bilayer and protein coat. Constituents of this protein coat, including butyrophilin 1a1 (Btn1a1) and xanthine dehydrogenase/ oxidase (Xdh/Xo), are presumed to function in milk-lipid secretion. We postulate that Btn1a1 is targeted to the apical membrane and binds to Xdh/Xo, which is present on the surface of intracellular lipid droplets. To determine the distribution of Btn1a1 and Xdh/Xo in lactating mammary tissue, we introduced recombinant adenoviral vectors encoding Btn1a1 or Xdh/Xo fused to variants of green fluorescent protein (GFP) into mouse mammary gland. The distribution of the respective expressed fusion proteins was determined by confocal microscopy. Results showed that Btn1a1 and Xdh/Xo were targeted to the apical plasma membrane and the surface of intracellular lipid droplets, respectively. Study of the distribution of either fusion proteins in the secreted droplets showed that the membrane forms crescent-like and blebbing structures, thus confirming earlier electron microscopic data, which suggested that the milk-lipid droplet membrane undergoes structural rearrangement after secretion.

EXPRESSION AND DISTRIBUTION OF BUTYROPHILIN 1A1 AND  
XANTHINE DEHYDROGENASE-OXIDASE IN LACTATING MAMMARY  
GLAND

By

Li Tao

Thesis submitted to the Faculty of the Graduate School of the  
University of Maryland, College Park, in partial fulfillment  
of the requirements for the degree of  
Master of Science  
2006

Advisory Committee:  
Professor Ian. H. Mather, Chair  
Professor Stephen Wolniak  
Associate Professor Wenxia Song

© Copyright by  
Li Tao  
2006

## Dedication

I dedicate this thesis to my parents.

## Acknowledgements

I am extremely thankful to my advisor, Dr. Ian Mather. He has been a consistent help throughout my years as a graduate student in his laboratory. Dr. Mather has taught me all the necessary techniques for this thesis research as well as the need to be persistent to pursue any goal in academic research. He was always there to help me solve problems that I encountered with in the research and in writing the thesis. I thank Dr. Jerry Schaack for preparing the adenoviral vectors, and Dr. Bob Brown and Dr. Iqbal Hamza for their help with the fluorescence microscopy. Dr. Wenxia Song and Dr. Stephen Wolniak have been a great help as committee members. I am thankful to Tanya Russell, Melissa Winn, Dr. Anita Rao, Dale Hailey, and Tim Mangel for their technical help. I also thank Liane Langbehn for animal care, and Anne Weldon, who has been a supportive colleague showing me histology techniques as well as a good friend off work. Special thanks to my friends Ying, Yi, Hui, and Caiyong for giving me a wonderful time in Maryland, and Ping, who makes the years worthwhile. Most of all, I thank my mother for her support and being the lifetime best friend for me; I regret that I could not be at my father's side when he was sick, I thank him for his love.

## Table of Contents

|   |      |
|---|------|
| Dedication.....   | ii   |
| Acknowledgements.....   | iii  |
| Table of Contents.....  | iv   |
| List of Tables.....   | v    |
| List of Figures.....  | vi   |
| List of Abbreviations.....                                    | viii |
| Introduction.....   | 1    |
| Materials and Methods:.....                                   | 20   |
| Materials:.....   | 20   |
| Methods:.....   | 21   |
| Storage of vectors.....                                       | 21   |
| Cell culture and transduction with adenoviral vectors.....    | 21   |
| Lysis and harvest of transduced HEK293 cells.....             | 22   |
| Transduction of mouse mammary glands <i>in vivo</i> .....     | 22   |
| Collection of milk.....                                       | 23   |
| Collection of mouse mammary tissues.....                      | 24   |
| Protein determination.....                                    | 24   |
| SDS/ Polyacrylamide gel electrophoresis and Western blot..... | 24   |
| Histology.....  | 25   |
| Results.....  | 26   |
| Discussion.....   | 56   |
| References.....   | 61   |

## List of Tables

|   |    |
|---|----|
| Table 1: Summary of mice infused with adenoviral vector ..... | 43 |
|---|----|

## List of Figures

|   |    |
|---|----|
| Figure 1. Three major pathways of lipid droplet transit and secretion from mammary epithelial cells .....                                   | 6  |
| Figure 2. The two major proposed mechanisms of milk-lipid droplet secretion from the apical membrane of mammary epithelial cells .....      | 8  |
| Figure 3. Electron microscopy of lipid secretion and MLGM formation.....  | 10 |
| Figure 4. Model of reconfiguration of MLGM and fat globule interactions after secretion .....   | 11 |
| Figure 5. Predicted topology of major proteins in MLGM.....   | 13 |
| Figure 6. Electron micrographs of lactating mammary tissue from Btn <sup>+/+</sup> , Btn <sup>+/-</sup> , and Btn <sup>-/-</sup> mice ..... | 14 |
| Figure 7. Mammary tissue from heterozygous mice deficient in Xdh/Xo. ....   | 17 |
| Figure 8. Postulated hypothesis for the secretion of lipid droplets from mammary epithelial cells .....                                     | 18 |
| Figure 9. Construction of Expression Plasmids and Adenoviral Vectors.....   | 28 |
| Figure 10. Western blot of fusion proteins expressed in HEK293 cells.....   | 30 |
| Figure 11. Transduction of HEK293 cells with Adv-BTN-EYFP adenoviral vector. ....   | 32 |
| Figure 12. Transduction of HEK293 cells with Adv-XDH-EYFP adenoviral vector .....   | 33 |
| Figure 13. Expressed fusion proteins of Xdh/Xo and Btn1a1 with EYFP in HEK293 cells, transduced with Adv-XDH-EYFP or Adv-BTN-EYFP .....     | 35 |
| Figure 14. Distribution of fusion proteins Btn-EYFP and Xdh-EYFP in HEK293 cells .....  | 36 |
| Figure 15. Fluorescence microscopy of milk-lipid droplets from mouse mammary gland transduced with Adv-XDH-EYFP .....                       | 39 |
| Figure 16. Fluorescence microscopy of milk-lipid droplets from mouse mammary gland transduced with Adv-BTN-EYFP .....                       | 41 |
| Figure 17. Expression of Xdh-EYFP in whole mouse mammary gland transduced with Adv-XDH-EYFP .....   | 44 |

|  |    |
|--|----|
| Figure 18. Expression of Btn-EYFP in whole mouse mammary gland transduced with Adv-BTN-EYFP .....                                      | 45 |
| Figure 19. Expression of Btn-EYFP and Xdh-EYFP in mouse mammary gland tissue transduced with either Adv-BTN-EYFP or Adv-XDH-EYFP. .... | 46 |
| Figure 20. Distribution of Btn-EYFP in mouse mammary gland transduced with Adv-BTN-EYFP. ....  | 47 |
| Figure 21. Distribution of Xdh-EYFP in mouse mammary gland transduced with Adv-XDH-EYFP.....   | 48 |
| Figure 22. Distribution of Btn-EYFP in secreted milk-lipid droplets .....  | 50 |
| Figure 23. Distribution of Xdh-EYFP in secreted milk-lipid droplets .....  | 51 |
| Figure 24. Z-stack confocal micrographs of Xdh-EYFP labeled lipid droplet.....   | 52 |
| Figure 25. 3-Dimensional reconstruction of Xdh-EYFP labeled lipid droplet.....   | 53 |
| Figure 26. Z-stack confocal micrographs of Btn-EYFP labeled lipid droplet.....   | 54 |
| Figure 27. 3-Dimensional reconstruction of Btn-EYFP labeled lipid droplet.....   | 55 |

## List of Abbreviations

|          |   |
|----------|---|
| Btn1a1   | mouse butyrophilin 1a1                                  |
| BSA      | bovine serum albumin                                    |
| CLD      | cytoplasmic lipid droplet                               |
| FLIP     | fluorescence loss in photobleaching                     |
| FRAP     | fluorescence recovery after photobleaching              |
| FRET     | fluorescence resonance energy transfer                  |
| GST      | glutathione-S-transferase                               |
| Ig       | immunoglobulin  |
| MLGM     | milk-lipid globule membrane                             |
| MLD      | microlipid droplet                                      |
| PBS      | phosphate-buffered saline                               |
| pfu      | plaque forming unit                                     |
| SDS      | sodium dodecyl sulfate                                  |
| SDS/PAGE | SDS/ polyacrylamide gel electrophoresis                 |
| TBS      | Tris-buffered saline                                    |
| TLCK     | Na- <i>p</i> -tosyl-L-lysine chloromethyl ketone        |
| TPCK     | Na- <i>p</i> -tosyl-L-phenylalanine chloromethyl ketone |
| Xdh/Xo   | mouse xanthine dehydrogenase/xanthine oxidase           |

## Introduction

Mammals are distinguished from other vertebrates because they have mammary glands, which are skin glands that secrete milk solely for the sustenance of their young. Lactation is the crucial time for the post-partum survival of neonates (1) and in the first several weeks to months of their life, milk is their only source of nutrients and water. Major milk components include water, ions, proteins, lactose, fat, and immunoglobulins. The composition of milk may vary because of species, diet, breed, genetics, mastitis, stage of lactation, as well as environmental conditions and many other factors. For example, seals have a comparatively high amount of fat and low quantities of water in their milks, which allows the mother to provide large amounts of energy for her young with a minimal expenditure of water, so that the young keep body temperature and grow rapidly in cold climates.

Raw whole milk can be separated into skim milk and cream by low-speed centrifugation. Generally the milk is first defatted (the cream is removed) at low centrifugal forces (about 5,000 to 10,000  $\times g_{av}$ , for 10 min), to prepare skim milk, which contains soluble proteins, casein micelles, ions, carbohydrates and water. If the skim milk is centrifuged at higher  $g$  forces, the casein, which is in the form of micelles, sediments as a white pellet, leaving a soluble fraction, which is called whey. The whey fraction contains soluble proteins, carbohydrate, water and minerals.

Major development of the mammary gland occurs during gestation and differentiation of the alveolar epithelium leads to the copious secretion of milk at the onset of parturition. The mammary gland is one of few tissues that can repeatedly undergo growth, functional differentiation, and involution during adult life.

Mammary gland development is initiated in the early fetal stage, continues around the time of puberty, and develops to a peak during late pregnancy. A single-layered sheet of cells derived from ectoderm forms a mammary band, which gives rise to the mammary buds at early stages of embryological development, followed by a dense mesenchyme. In the mouse, stromal cells develop from the mesenchyme and become a fat pad, which consists mostly of adipocytes, fibroblasts, nerves, and blood vessels. The streak canal, teat, and gland cisterns begin to form from the mammary bud. Essentially at birth the gland consists of a limited duct system penetrating into adipose and connective tissue. Most mammary development takes place during gestation, and the greatest promoters of mammary growth are the hormones of pregnancy. Depending upon species, major hormones include estrogen, which is required for ductal development, progesterone, which is required for alveolar morphogenesis, and prolactin, which is required for lactogenesis. During this time, extensive arborization of the ductal system and formation of lobulo-alveolar structures take place and the mammary gland is eventually filled with alveoli. Mammary epithelial cells are fully differentiated at parturition and become polarized with a basolateral region, a Golgi complex, and apical cytoplasm filled with secretory vesicles and lipid droplets (2).

Two major cell-types are responsible for the production and removal of milk from the gland: secretory epithelial cells and myoepithelial cells. The former line the alveolar luminae and secrete all of the major components of milk. The later are located beneath the secretory epithelium and function in milk-ejection. The milk ejection reflex involves the oxytocin-induced contraction of the myoepithelial cells to

increase internal pressure within the alveolus and force stored secretions into the ducts and subsequently to the nipple.

Mammary growth continues during the early days of lactation in many species. In mouse, there is a transient surge in mammary cell proliferation 2 to 3 days postpartum. This is consistent with the results in this thesis, in which we detected the highest levels of expressed recombinant protein during early lactation. However, increased growth after parturition is prevented if suckling is not permitted in most species and the gland undergoes premature involution.

The mammary gland reverts to a virgin status morphologically when the neonates are weaned unless there is the stimulation of another pregnancy. The secretory epithelial cells undergo apoptosis, and the gland alveolar structure is eventually degraded (3). Involution can be stimulated at any stage of lactation by removal of the suckling neonates. Further cycles of mammary gland proliferation and differentiation occur at the onset of succeeding pregnancies (2).

Although the proportion of each constituent differs among species, due to the different needs of the neonate and nature of the environment, the qualitative composition of milk is very similar among mammals. Lipid droplets, caseins, lactose and water are major constituents in nearly all species. Lactose is the major carbohydrate in most milks (4). Besides providing digestible carbohydrate, it also plays a major role in controlling the osmotic balance between milk and mammary secretory epithelial cells by drawing water into milk across the secretory vesicle membranes and the apical surface (5). All milks contain protein, which as discussed above, can be separated by centrifugation into casein and whey fractions.

Caseins comprise up to 80% of total milk protein in cows (6) and are in the form of micelles. The  $\alpha$ -casein and  $\beta$ -caseins are calcium-binding proteins, which form the core of the micelle, with  $\kappa$ -casein surrounding the outer surface. Milk fat is also a component conserved in all milks. The major lipids in milk are triacylglycerols, which are secreted as fat globules covered with a protein coat and a bilayer membrane of phospholipids and integral and peripheral proteins. The protein coat and the bilayer membrane are collectively called the milk-lipid-globule- membrane (MLGM) (7). The potential role that major protein constituents of the MLGM may play in the secretion of milk-lipid droplets is the subject of this thesis.

Both the integral and peripheral proteins of the MLGM may play important roles in coating and stabilizing newly synthesized fat droplets and milk-lipid droplets. Major proteins of the membrane include the redox enzyme xanthine dehydrogenase/oxidase (Xdh/Xo), butyrophilin 1a1 (Btn 1a1), mucin 1 (MUC1), mucin 15B, lactadherin, CD36, adipocyte differentiation-related-protein (ADRP) or adipophilin (ADPH) (reviewed in (8)). Two major MLGM proteins, the membrane protein butyrophilin 1a1 (Btn 1a1) and the soluble protein xanthine dehydrogenase / oxidase (Xdh/Xo) have been proposed to play a functional role in milk-lipid secretion and they are the major focus of this thesis research (9).

Triacylglycerols are the principal components of cream in milks and comprise up to 97% of the total lipids in cows' milk (10, 11). Lipids are also present in the skim milk as membrane fragments (12). In origin, lipid is first formed as small droplets on the membranes of the rER (10, 11, 13, 14), although the exact location of lipid synthesis is still unknown. Possible locations could be the cytoplasmic surface,

luminal surface or between the bilayer membrane (6, 9, 13). In one point of view, lipid molecules nucleate during synthesis on the cytoplasmic surface to form small droplets, which are directly released into the cytoplasm (14). Some membrane proteins, such as Btn1a1, are presumed to be excluded from the covering of the microlipid droplets, whereas other proteins, including ADPH and lipids such as glycerophospholipids become incorporated into the surface coat of the droplets (15, 16).

Following release into the cytoplasm, the newly synthesized lipid droplets, which at this stage are called microlipid droplets (MLDs) (17) migrate toward the apical plasma membrane by unknown mechanisms. Elements of the cytoskeleton including microtubules and actin may play major roles (18). Some of the MLDs, which are small in size (diameters less than 0.5  $\mu\text{m}$ ), fuse together and form bigger droplets during transport to the apical pole of the cell. The fused and enlarged lipid droplets are called cytoplasmic lipid droplets (CLDs). CLDs are considered to be the direct precursors of large milk-lipid droplets, while MLDs are assumed to give rise to the small lipid globules in milk (15). Separation of MLDs and CLDs shows that they have similar coat compositions, which presumably reflects their common origin in the rER (15, 19).

Fat droplets are secreted into the alveolar lumen after targeting to the apical membrane of mammary epithelial cells. Three pathways have been proposed. MLDs, which do not fuse with other MLDs or CLDs and do not enlarge in size, migrate to the apical pole and are gradually coated with plasma membrane and secreted from the apical surface directly (**Figure 1**). These MLDs comprise the small droplets in milk.

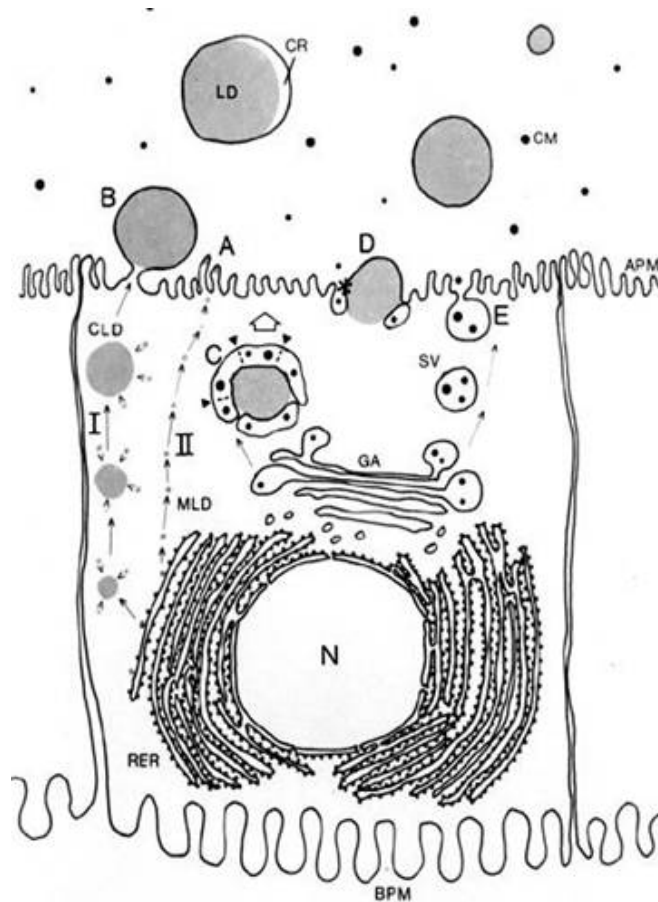


**Figure 1. Three major pathways of lipid droplet transit and secretion from mammary epithelial cells**

MLDs are synthesized in the rER and move to the apical surface. I: MLDs fuse with each other and form larger CLDs as they are transported to the apical surface, where they are secreted as CLDs (B). II: The MLDs are transported to the apical surface without changing their size and are secreted as MLDs (A). III: The CLDs are surrounded by secretory vesicles, which form intracytoplasmic vacuoles around the fat droplets in the cytoplasm. After fusing with the apical PM the fat droplet is exocytosed from the cell (C). D shows a combination of secretory mechanisms B and C. Casein and other milk components are secreted by exocytosis from secretory vesicles at the apical PM (E). Apical plasma membrane (APM); basal plasma membrane (BPM); cytoplasmic crescent (CR); rough endoplasmic reticulum (RER); lipid droplet (LD); Golgi apparatus (GA); cytoplasmic lipid droplet (CLD); microlipid droplet (MLD); nucleus (N); secretory vesicle (SV). Figure and legend reproduced from (9) with permission.

In an alternative pathway the CLDs enlarge dramatically in the apical pole of the cell by continued fusion with smaller droplets and are surrounded with apical plasma membrane until a narrow neck is formed. After the neck fuses together and seals, the droplets are released into the lumen. The enlarged CLDs comprise the large droplets in milk (20). In this mechanism some of the droplets acquire cytoplasmic inclusions, which have a crescent-like appearance in electron micrographs of secreted milk-lipid droplets. Such cytoplasmic inclusions are much more common in some species, e.g., rabbit and human, than others, e.g., cow and guinea pig (21). In a very different view, the lipid droplets are presumed to associate with secretory vesicles from the Golgi apparatus in the apical pole of the cell (22, 23). The secretory vesicles either partially or completely surround the droplets and the membranes of the vesicles fuse together to form a cytoplasmic vacuole. The contents of such vesicles are then released from the apical surface by exocytosis (**Figure 1**). A combination of both mechanisms has also been proposed (**Figure 2**).

The actual mechanism of milk-lipid droplet secretion at the molecular level has not yet been established. It is not clear how the droplets fuse, how lipid droplets are transported to the apical membrane, what forces are involved in the targeting, and how the droplets acquire the outer coat of membrane during secretion. Several mechanisms of milk-lipid secretion have been proposed (9). Our aim is to test the most accepted model:-that milk-lipid droplets bind to the apical membrane through interactions between membrane- and lipid-droplet- associated proteins, and that these proteins are secreted with the lipid in the MLGM (9, 16).

In the process of lipid droplet targeting to, and budding from, the apical

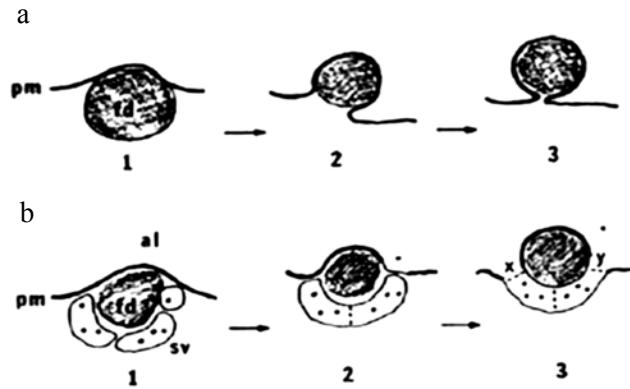


**Figure 2. The two major proposed mechanisms of milk-lipid droplet secretion from the apical membrane of mammary epithelial cells**

(a), 1, apical plasma membrane surrounds the fat droplet. 2, a neck forms. 3, neck narrows and finally fuses. (b), 1, secretory vesicles from the Golgi apparatus surround fat droplets together with the apical plasma membrane; 2, membranes of the secretory vesicles fuse with each other and with the plasma membrane; 3, after secretory vesicle and plasma membrane fusion, the fat droplets are secreted. Figure and legend reproduced from (6) with permission.

membrane, the droplet remains a constant distance of about 10-20 nm from the outer membrane bilayer (22) (**Figure 3a**). This layer consists of protein, and appears as a fuzzy electron dense coat in electron micrographs of isolated membrane (24) (**Figure 3c**). Freeze-etch electron microscopy has shown that areas of the protein coat appear as a very ordered paracrystalline structure with hexagonal symmetry in freeze-etched preparations (25) (**Figure 3b**).

Immediately after milk secretion, the bilayer membrane uniformly covers the milk-lipid droplet surface (22). However in fixed specimens the structure of the MLGM alters in the luminae of alveoli and ducts, and the membrane appears to be structurally rearranged (23, 24, 26) (**Figure 4**). The inner surface of the membrane bilayer of the MLGM and the outer surface of the lipid droplet tend to fuse, forming areas of apolar contact. Expansion of the contact zones between the two surfaces leads to the formation of intervening areas, in which the protein coat is condensed (22) and the outer membrane bilayer blebs off in the form of vesicles carrying the amorphous coat derived from the surface of the droplet (12, 24). The extent that this vesiculation process occurs *in vivo* has been questioned because of the difficulty of chemically fixing membrane-coated lipid droplets for electron microscopy (9). Data obtained during this current research project directly addresses this issue.

The mechanism of MLGM formation has attracted much interest. Mather and Keenan have suggested that MLGM proteins play an important role in lipid-droplet secretion and proposed a working hypothesis on which this thesis research is based.

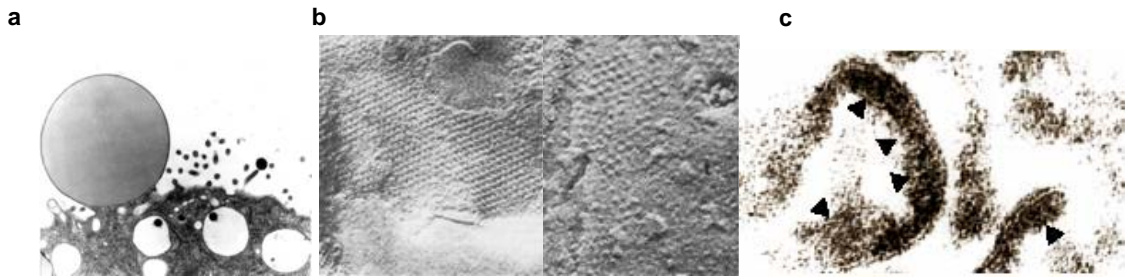


**Figure 3. Electron microscopy of lipid secretion and MLGM formation**

a, Lipid droplet budding out from the apical surface of secretory cell (Mather, I. H., unpublished observations) b, Freeze-etch microscopy of inner surface of MLGM showing protein coat with hexagonal symmetry (25). c, Electron micrograph of MLGM showing electron dense coat on inner face of membrane (arrowheads) (27).

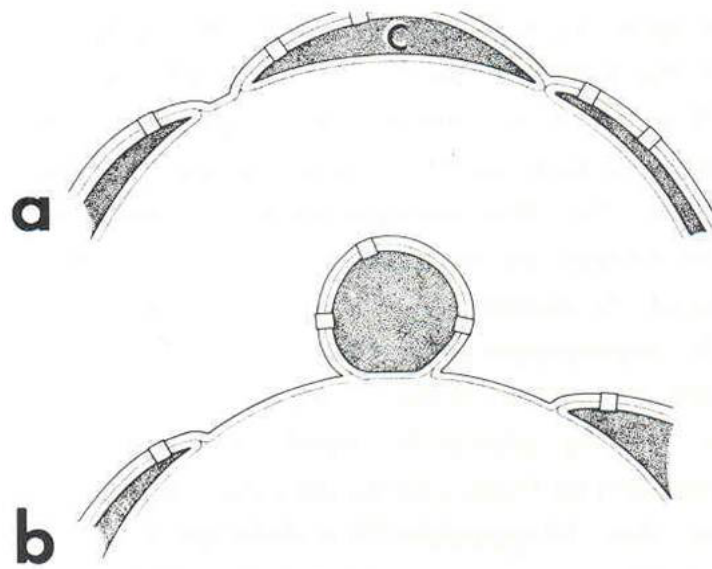


**Figure 4. Model of reconfiguration of MLGM and fat globule interactions after secretion**

The inner surface of the bilayer membrane and outer surface of the lipid droplets may interact with each other after secretion. Crescents, caps, and blebs may form. a, formation of crescent-like areas (c); b, membrane blebbing. Adapted from ref. (28).

In this hypothesis it is proposed that proteins on the surface of the intracellular lipid droplet and proteins in the apical plasma membrane interact and bind to each other as an initial step in the formation of the MLGM. Potential interacting partners include Btn1a1, microtubules, Xdh/Xo and ADPH. An analysis of the topology of the MLGM from washed fat globules (29) and other considerations (9) suggest that Btn1a1 and Xdh/Xo may play a major role in formation of the MLGM and these proteins are discussed separately below.

Butyrophilin (Btn1a1) is the only major protein of the MLGM with a cytoplasmic tail long enough to bind with other proteins (**Figure 5**). Btn1a1 is also one of the most abundant proteins in the MLGM in many species including human and cow (30, 31) and it is specifically expressed in lactating mammary gland (32), especially during lactation, and also immediately preceding the onset and following the cessation of lactation. Most importantly, knock-out of the butyrophilin gene in mice causes disruption of MLGM structure and regulated milk-lipid secretion (33) (**Figure 6**), providing direct evidence that Btn1a1 functions at same stage in milk-lipid secretion.

Btn1a1 forms one of a subfamily of ten genes in the immunoglobulin (Ig) superfamily, identified in human, mouse and other species (35-37). The structure of most Btns comprises two Ig-folds in the exoplasmic domain, a single membrane anchor, and a B30.2 domain, which is the predominant part of the cytoplasmic domain (38). A recent X-ray crystal structure study shows that this domain has multiple  $\beta$  strands, and comprises a  $\beta$  sandwich and is similarly present in many other proteins (39, 40).

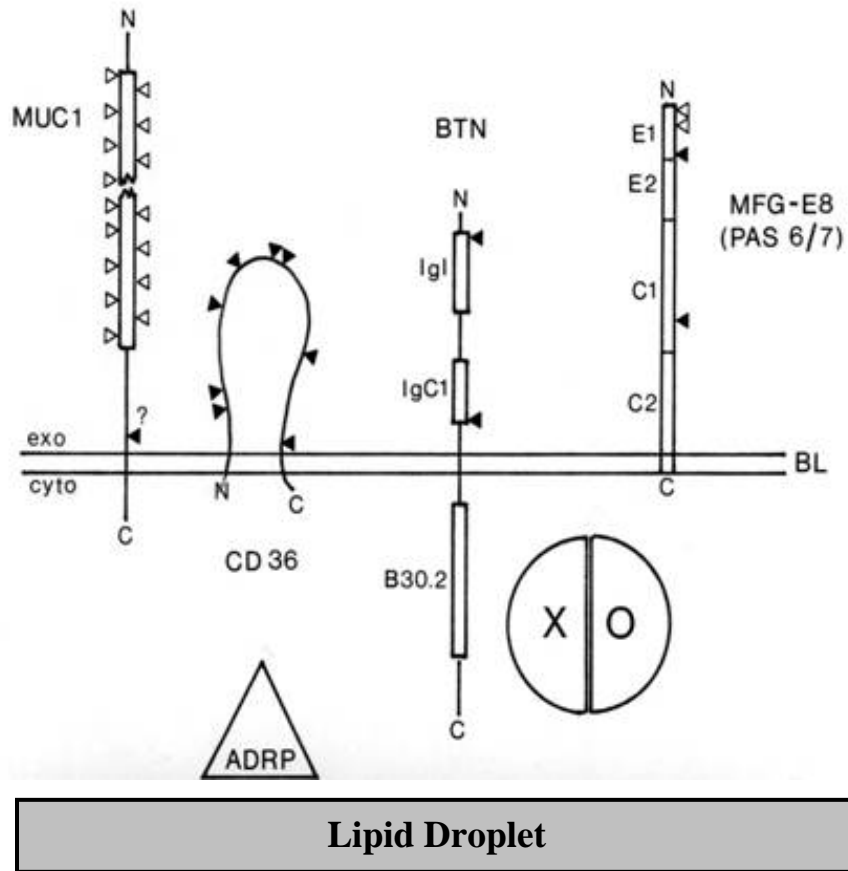


**Figure 5. Predicted topology of major proteins in MLGM**

Integral proteins include MUC1, CD36 and BTN. MUC1 and BTN are type 1 membrane proteins with the N-termini on the exoplasmic side and C-termini on the cytoplasmic side. BTN is a member of the immunoglobulin superfamily with two immunoglobulin-like domains (IgI, IgC1) and a single cytoplasmic tail. XO (xanthine oxidase) and ADRP (adipophilin) are peripheral membrane proteins that do not have membrane anchors. These two proteins are probably associated with the cytoplasmic face of MLGM (9).

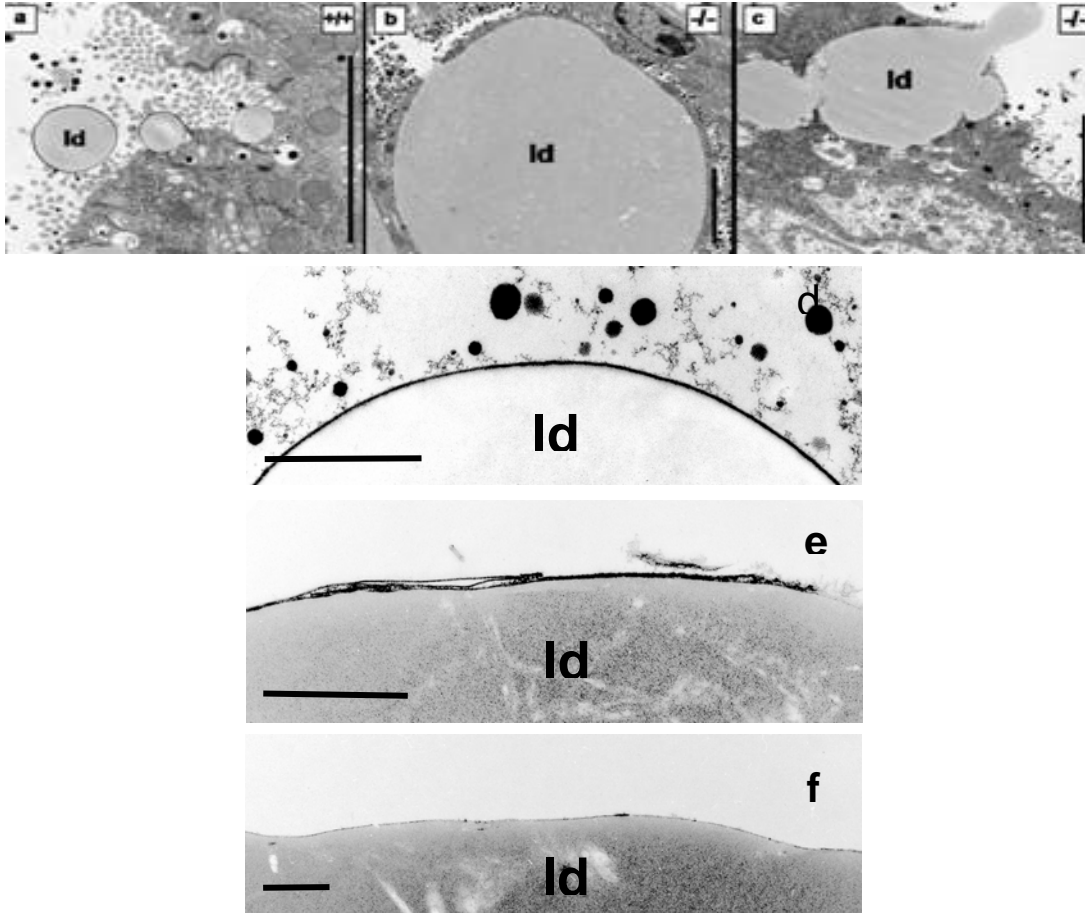


**Figure 6. Electron micrographs of lactating mammary tissue from  $Btn^{+/+}$ ,  $Btn^{+/-}$ , and  $Btn^{-/-}$  mice**

(a-c) secretory epithelial cells; (e-f) MLGM on lipid droplets in milk. (a), (d) micrographs of tissue and lipid droplets of wild type mice; (b), (c), (e), (f): micrographs of tissue and lipid droplets of knock-out mice; (b), (c): lipid droplets are not synthesized and secreted normally in knock-out mice compared to wild type; (e), (f): MLGM is discontinuous and disrupted in knock out mice (33). (a-c) bars  $5\mu\text{m}$ , (d-e) bars  $1\mu\text{m}$ .

Xanthine dehydrogenase/oxidase (Xdh/Xo or Xdh) may be linked to milk-lipid secretory activities because it binds to Btn1a1 (41). Xdh/Xo is one of the most abundant proteins in the MLGM in many species and is highly expressed, as a soluble protein, in lactating mammary tissue (42, 43).

Xdh/Xo is a redox enzyme that is widely distributed in many tissues in mammals and functions in purine metabolism. Xdh/Xo is a homodimer with an aggregate molecular weight of 300,000 Da. Each monomer has four domains, two  $Fe_2/S_2$  domains at the N-terminus, a central flavin binding domain, and a C-terminal molybdopterin binding domain (44). Two forms of Xdh/Xo are present in mammals: an oxidase and a dehydrogenase. The dehydrogenase preferentially utilizes  $NAD^+$  as electron acceptor, which is converted to  $NADH^+/H^+$ . The oxidase form transfers electrons from the reduced enzyme to molecular oxygen, which is converted to hydrogen peroxide and superoxide radicals. Purines bind to the enzyme at the molybdopterin site, and  $NAD^+$ /oxygen interacts with the  $FAD^+$  domain. Xdh/Xo can be converted into the oxidase form by oxidation of key sulfhydryl residues (45).

Structurally, Xdh/Xo is a butterfly shaped dimer (46). Because the distance between the two monomers is not close enough for electron transfer to occur, each of the monomers is catalytically independent. In the mammary gland, Xdh/Xo expression is significantly increased during pregnancy and becomes maximal around mid-lactation, which suggests an important role in milk synthesis or secretion (47). Furthermore, lactating mammary glands have higher levels of Xdh/Xo compared to most other mammalian tissues (48). Thus, although the reported main function of Xdh/Xo is in the oxidation of purines, in the mammary gland Xdh/Xo may have other functions

related to lactation. Xdh/Xo has been detected in both the cytoplasm and the apical surface of mammary epithelial cells during lactation (49). Most significantly, the Xdh/Xo<sup>+/-</sup> heterozygote has a very similar lactation phenotype to that of the Btn<sup>-/-</sup> mouse; secretion is disrupted and lipid droplets accumulate in the cytoplasm (**Figure 7**). Milk contains fewer fat droplets in the Xdh/Xo<sup>+/-</sup> mice, than milk from wild-type mice (47). These results provide direct evidence that the normal expression of Xdh/Xo is required for regulated lipid secretion. [Note: The lactation phenotype of the homozygous knock-out Xdh/Xo mouse (Xdh/Xo<sup>-/-</sup>) cannot be analyzed because the mice do not live beyond 6 weeks of age].

Although these above results imply that Btn1a1 and Xdh/Xo may function in milk-lipid secretion, many major questions still remain unanswered in the field. These questions include: what is the distribution of Btn1a1 and Xdh/Xo in mammary secretory epithelial cells, what is the targeting mechanism of milk-lipid droplets to the apical membrane, and is interaction between Btn1a1 and Xdh/Xo essential for lipid secretion? Based on the available data we propose the following working hypothesis: Btn1a1 is synthesized and processed through the secretory pathway and located on the apical membrane while Xdh/Xo is synthesized in the cytoplasm and distributed to the surface of intracellular lipid droplets, during their transport to the apical pole of the cell. Btn1a1 self-associates in the plane of the apical membrane and binds to Xdh/Xo thus bringing the lipid droplets in contact with the membrane bilayer and initiating formation of the MLGM. Further interactions between Btn1a1 and Xdh/Xo lead to the gradual expulsion of the droplets from the cell (**Figure 8**).

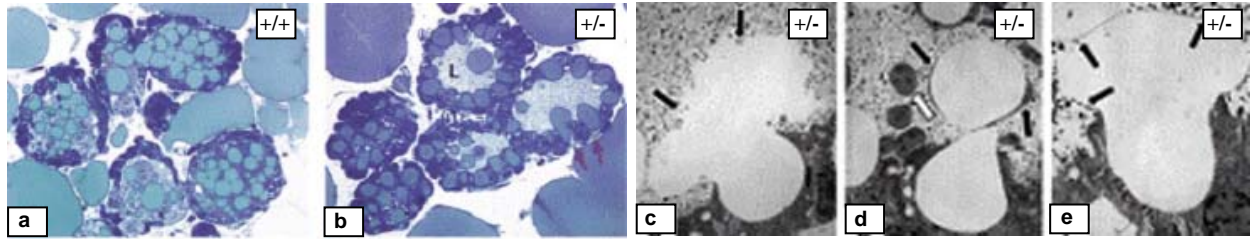


**Figure 7. Mammary tissue from heterozygous mice deficient in *Xdh/Xo*.**

Histological analysis of resin-embedded mammary glands of wild-type and *Xdh*<sup>+/-</sup> mice. The arrows indicate epithelial cells in which accumulated fat droplets appear to break out from the apical outface of the cell. (a-b) light micrographs; (c-e) electron micrographs show disruption of lipid droplets, similar to that caused by a deficiency in *Btn1a1* (50).

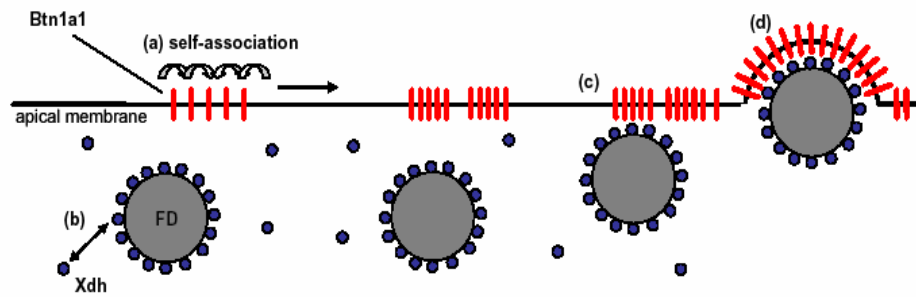


**Figure 8. Postulated hypothesis for the secretion of lipid droplets from mammary epithelial cells**

(a) Btn1a1 self-associates in the form of tetrameric/ pentameric complexes in the apical plasma membrane. (b) Xdh is synthesized in the cytoplasm, binds to the surface of milk-lipid droplets, and is transported together with the lipid droplets to the apical pole of the cell. (c) Xdh on the surface of the lipid droplets binds with multimeric forms of Btn1a1, bringing the lipid droplets to the apical membrane bilayer and initiates formation of the MLGM. (d) Further interactions between Btn1a1 and Xdh lead to expulsion of the lipid droplets from the cell.

Recent advances in the *in vivo* expression of recombinant protein allow us to test several aspects of this hypothesis. The mammary gland provides a good model for *in vivo* study, because the gland parenchyma is directly accessible through the mammary duct in the nipple, thus allowing the introduction of vectors encoding target genes to express recombinant proteins of interest. Investigators have taken advantage of such intraductal injection techniques to study the permeability of the mammary epithelium to ions and sucrose in goats and mice (51), and DEAE-dextran-mediated transfection was used to express reporter proteins including human growth hormone in the guinea pig mammary gland (52). More recently, adenoviral vectors encoding a green fluorescent protein (GFP) reporter were injected intraductally into the mouse mammary gland to evaluate transduction efficiency (53).

In this thesis research, we used adenoviral vectors to explore our questions about milk-lipid secretion in mammary epithelium cells. Adenoviral vectors were constructed encoding fusion proteins of either wild type Btn1a1 or Xdh/Xo with a fluorescence tag comprising enhanced yellow fluorescent protein (EYFP). The expressed recombinant forms of Btn1a1 and Xdh/Xo were fused with the fluorescence tag at the respective C-termini. We discuss the transduction of the mouse mammary gland with adenoviral vectors encoding these constructs. Optimal conditions for infusion of the vectors and expression of the proteins were tested. The steady-state distributions of the Btn1a1 and Xdh/Xo fusion proteins were determined by microscopy of fixed tissue and freshly collected milk samples.

## Materials and Methods:

### Materials:

RPMI 1640, trypsin-EDTA and penicillin streptomycin fungizone (PSF) were from Gibco (Gaithersburg, MD). Fetal calf serum was from Atlanta Biologics (Atlanta, GA). Mowiol was from CalBiochem (La Jolla, CA). Tris, sodium dodecyl sulphate (SDS), ammonium persulphate, N,N,N',N' tetramethylethylenediamine (TEMED), goat anti-(rabbit-IgG) conjugated to horse-radish peroxidase, gelatin, nitrocellulose, ampholines, bromophenol blue, Coomassie brilliant blue R-250, acrylamide, N,N' methylenebisacrylamide, and Triton X-100 were obtained from Bio-Rad Laboratories (New York, NY). Bicinchoninic acid (BCA) and bovine serum albumin (BSA) were from Pierce Chemical Company (Rockford, IL). ECL™ Western blotting detection reagents and Hyperfilm™ were obtained from Amersham Life Sciences (Buckinghamshire, England). Rabbit anti-GFP IgG was from Molecular Probes (Eugene, Oregon). Mouse mammary gland infusion micropipettes were obtained from Drummond Scientific (Broomall, PA). O.C.T. Compound was from Tissue-Tek (Torrance, CA). All other chemicals and reagents were from Fisher (Pittsburg, PA).

Adenoviral vectors were constructed in the laboratory of Dr. Jerry Schaack (University of Colorado, University of the Health Sciences, Denver, CO).

## Methods:

### Storage of vectors

For long-term storage, stocks of each adenoviral vector were kept in storage buffer (10 mM Tris-HCl, pH 7.5, 10 mM histidine, 75 mM NaCl, 1 mM MgCl<sub>2</sub>, 100 μM EDTA, 0.5% v/v EtOH, 50% v/v glycerol) at -80°C. Working stocks of each vector were diluted to 2.7x10<sup>10</sup> pfu/ μl in the same buffer and stored at -20°C for a maximum of one month. Immediately before the infusion of adenoviral vectors into mouse mammary glands, vectors were diluted to 2.7x10<sup>7</sup> pfu/ μl in Krebs Ringer's buffer (138 mM NaCl, 8.1 mM Na<sub>2</sub>HPO<sub>4</sub>, 1.2 mM K<sub>2</sub>HPO<sub>4</sub>, 2.7 mM KH<sub>2</sub>PO<sub>4</sub>, 0.9 mM CaCl<sub>2</sub>, 0.5 mM MgCl<sub>2</sub>) and kept on ice before use.

### Cell culture and transduction with adenoviral vectors

HEK293 cells were grown on plastic tissue culture plates in RPMI 1640 medium containing 10% FBS and 1% penicillin/streptomycin/l-glutamate at 37°C in an atmosphere of 95% air and 5% CO<sub>2</sub>. HEK293 cells were grown to 60-80% confluency and were counted using a hemacytometer (Bright-Live, Buffalo, NY). Cells were transduced with adenoviral vectors by adding the diluted vectors from the working stocks (2.7 x 10<sup>7</sup> pfu/ μl) to the culture medium based on the amount of cells in each tissue culture plate, to ensure that fixed vector/cell ratios were applied. Vector titers ranging from 0.1 to 25 pfu/ cell were tested. Transduced cells were incubated overnight in the above culture conditions.

### Lysis and harvest of transduced HEK293 cells

Cells were washed three times with 3 ml of ice-cold Dulbecco's phosphate-buffered saline (D-PBS: CaCl<sub>2</sub>- and MgCl<sub>2</sub>- free, Sigma), scraped from the culture plate in 800 µl of D-PBS, and transferred to 1.5 ml eppendorf centrifuge tubes. The harvested cells were then centrifuged at 1,000 *g*<sub>av</sub> for 30 sec, the D-PBS was removed and the cells were resuspended in 250 µl lysis buffer (20 mM HEPES, pH 7.4, 150 mM NaCl). Cells were lysed by three consecutive rounds of freeze-thawing, firstly at -80°C and then on ice, and the lysates were then centrifuged at 15,000 *g*<sub>av</sub> for 30 min at 4°C. The lysate supernatants were collected and transferred to fresh microcentrifuge tubes, the pellets were resuspended with the same volume of lysate buffer and both fractions were stored at -20°C.

### Transduction of mouse mammary glands *in vivo*

Mice were anesthetized by the intraperitoneal injection of avertin at a dosage of 125 to 250 mg/ kg body weight and kept warm under the light of a microscope illuminator (Fisher). Glands were washed with 70% ethanol, and the hair was trimmed around the nipple to be infused. Glass micropipettes for infusion were prepared by pulling the glass tip over a Bunsen flame into a fine tip of 60 to 75 µm and the ends fire-polished to remove sharp edges.

A stock of adenoviral vector (2.7 x 10<sup>7</sup> pfu/ µl) was made by diluting the original adenoviral vector stock with storage buffer as above. Final doses (2.7 x 10<sup>7</sup> pfu for number 4 mammary glands; 2 x 10<sup>6</sup> pfu for number 3 mammary glands, as described by Russell. *et al*, (53) were made by diluting the 2.7 x 10<sup>7</sup> pfu/ µl stock

with 100  $\mu$ l of sterile filtered Ringer's solution. This dilution was made immediately before the infusion to ensure the stability of the vectors. The solution was loaded into a 25  $\mu$ l Wiretrol II disposable glass micropipette with a stainless steel plunger (no. 5-000-2050; Drummond Scientific Company, Broomall, PA). By using a micromanipulator (World Precision), the tip was gently inserted into the teat canal, and the solution was slowly injected into the luminal spaces of either the number 3 or number 4 mammary glands. Micropipettes were washed three times each with Ringer's solution, 70% ethanol and distilled water between each vector infusion. Each gland was infused four times with 25  $\mu$ l aliquots of vector, for a total of 100  $\mu$ l per gland.

#### Collection of milk

Mice were separated from their litters for approximately 3 h and were then injected i.p. with avertin (125 to 250 mg/ kg body weight) and 0.2 I.U. of oxytocin in physiological saline. Milk was collected with a hand-held vacuum device into capillary tubes as described by Teter, *et. al* (54). The milk was centrifuged for 15 min at 15,000  $g_{av}$  at room temperature in a hematocrit centrifuge and the fat and skim milk samples, partially cleared of casein, were collected by breaking the capillary tubes at the skim-milk/lipid interface. Milk was also spotted onto microscope slides after dilution with PBS and sealed under cover slips with nail polish to examine the fat droplets by fluorescence microscopy.

### Collection of mouse mammary tissues

Mice at either the 3<sup>rd</sup> day or the 20<sup>th</sup> day of lactation were asphyxiated by immersion in CO<sub>2</sub>. Mammary glands were rapidly excised, weighed, spread on a glass plate on top of ice to keep cold, and homogenized in 10 mM Tris- HCl, pH 7.2, 140 mM NaCl containing protease inhibitors (20 mM HEPES pH7.0 containing 150 mM NaCl, TPCK 0.125 mM, TLCK 0.125 mM, PMSF 1 mM, EACA 10 mM, and aprotinin 0.2 units). The tissue was minced finely and homogenized in a Dounce homogenizer in the above homogenization buffer containing protease inhibitors as described above. The homogenized tissue was then centrifuged at 15,000 *g<sub>av</sub>* for 10 min at 4° C. Pellets were resuspended with 200 µl of PBS.

### Protein determination

Protein was determined by the BCA<sup>TM</sup> protein assay (Pierce) according to the manufacturer's instructions, using bovine serum albumin as a standard (55).

### SDS/ Polyacrylamide gel electrophoresis and Western blot

SDS-PAGE was performed in 8% (w/v) acrylamide gels as described by Laemmli *et. al.*(56). Protein samples from cell lysates or homogenized tissue were prepared by heating at 95° C for 3 min in SDS-PAGE Laemmli buffer. Samples (10-20 µg protein) were separated for 3-4 h at a constant current of 30 mA/slab gel and then transferred to nitrocellulose membrane using the method of Towbin *et. al.* (57). Membranes were blocked with 5% dry milk/high-salt TBS (0.5M NaCl, 20 mM Tris-

HCL, pH 7.4) overnight and then incubated with diluted primary anti-GFP antibody for 1 h in 2.5% dried milk/Bio-Rad TBS. Anti-peptide rabbit polyclonal antibodies to the C-terminal amino acid residues of Btn1a1 were prepared as described by Ogg. *et al.* (33) and purified as described by Banghart *et al.* (29). The membranes were washed three times, firstly for 15 min, and then twice for 10 min each time, with high-salt TBS and then incubated with goat-anti-rabbit IgG conjugated to horseradish peroxidase (Bio-Rad blotting grade) for 1 h in 2.5% dried milk/high-salt TBS. The membranes were then washed again three times as described above. Chemiluminescence was used to detect immunoreactive protein, using the ECL kit from Amersham according to the manufacturer's directions.

### Histology

Mouse mammary glands were spread out onto microscope slides in Petri dishes, and covered with 4% (w/v) paraformaldehyde in PBS buffer, pH 7.25 and fixed overnight at 4°C. The whole gland was dissected into three major parts denoted as the nipple area and the medial and distal areas. Each of the fixed parts was chopped into 1mm pieces, which were placed in molds containing O.C.T. compound and then quick-frozen by holding them in liquid nitrogen. The embedded tissue was sectioned at a thickness of 6-8 µm using a Leica Frigocut 2800E cryomicrotome. The sectioned tissue was washed with PBS on microscope slides to remove O.C.T. compound and then mounted in Mowiol, protected with a coverslip, and examined with a Zeiss LSM 410 or 510 laser confocal microscope.

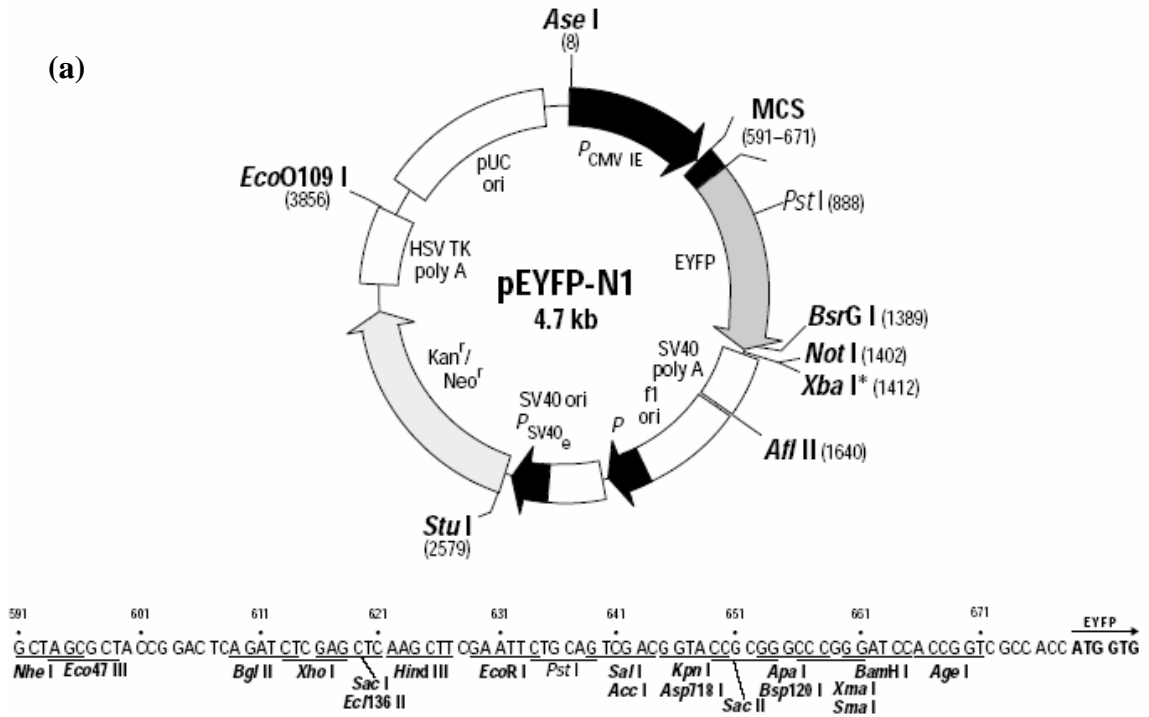
## Results

Based on the potential roles of Btn1a1 and Xdh/Xo in milk-lipid secretion, we focused on two research aims for this thesis research. Firstly, we tested the feasibility of expressing Btn1a1 or Xdh/Xo as fusion proteins with variants of GFP in HEK 293 cells using adenoviral vectors. Secondly, to study the distribution of Btn1a1 and Xdh/Xo in mammary epithelial cells and milk, we infused the adenoviral vectors into mouse mammary glands through the streak canal of the nipple and examined the distribution of the expressed proteins in tissue and milk by confocal microscopy.

As a first step towards constructing adenoviral vectors, recombinant plasmids encoding either Btn1a1 or Xdh/Xo fused with EYFP or ECFP respectively at the C-termini were made by Dr. I. Mather. The recombinant plasmids were based on the pEYFP-N1 plasmid from Clontech with mutations incorporated into the EYFP cDNA to prevent self-association of the expressed fluorophores (58). The respective cDNAs encoding each entire fusion protein were excised from the completed Clontech plasmids and used by Dr. J. Schaack to prepare adenoviral vectors (59). Plasmid and adenoviral vector construction is summarized in **Figure 9**. The plasmids were defined as pBTN-EYFP and pXDH-EYFP to indicate EYFP is fused to the C-terminus of Btn1a1 or Xdh/Xo in the fusion protein. The adenoviral vectors were defined as Adv-BTN-EYFP and Adv-Xdh-EYFP, respectively.

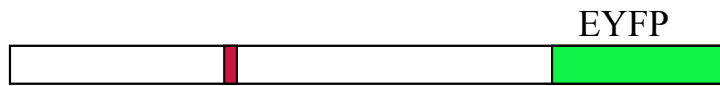
To test whether fusion proteins of Btn1a1 or Xdh/Xo with EYFP were expressed as full-length proteins, the respective plasmids were transfected into HEK293 cells. Western blot of cell lysates showed that the proteins were expressed as

(a)

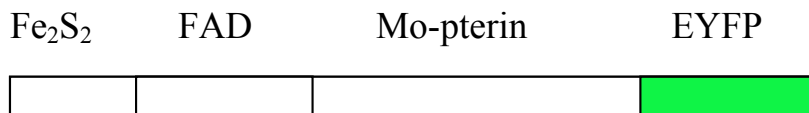


(b)

Btn1a1



Xdh



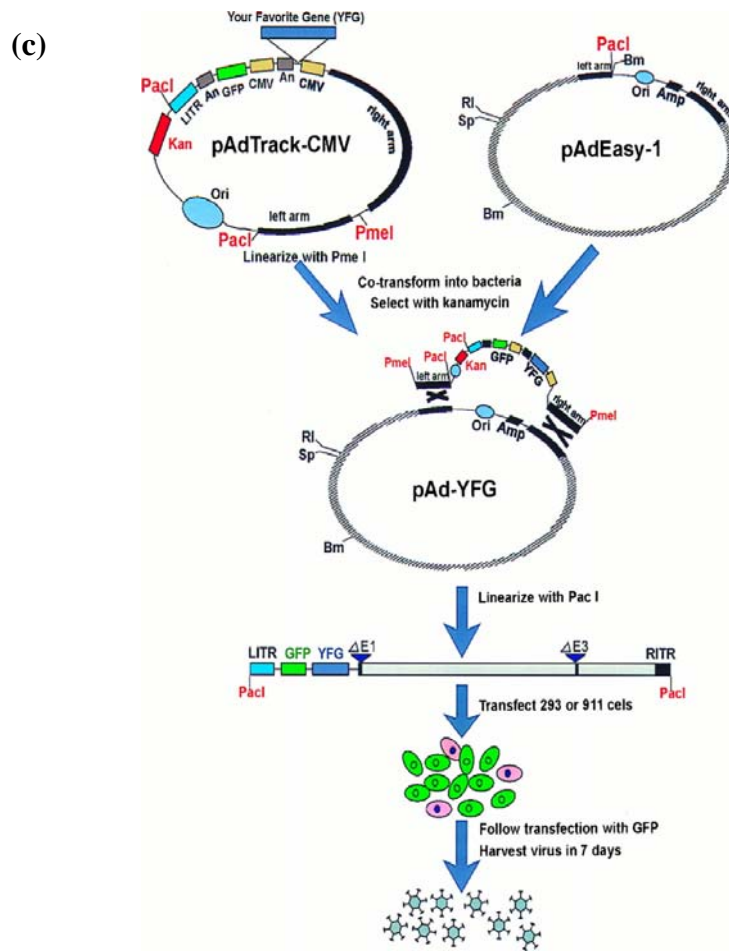


**Figure 9. Construction of Expression Plasmids and Adenoviral Vectors**

(a), Restriction map and multiple cloning site of pEYFP-N1 from Clontech. Unique restriction sites are in bold. The Xba I site (\*) is methylated in the DNA provided by Clontech. (b), Schematics of cDNAs encoding the respective fusion proteins inserted into pEYFP-N1. The cDNAs encoding either Btn1a1 or Xdh/ Xo were fused at the 3'-end to the 5' end of the cDNA for EYFP in the plasmid and then recovered by digestion with *Nhe*1 and *Not*1. (c), Adenoviral vector construction. cDNAs containing Btn1a1 or Xdh/ Xo cDNAs fused with EYFP were cloned into the pShuttle-CMV vector downstream of a CMV promoter. The construct was then cleaved with restriction endonuclease to linearize it and transformed together with adenoviral vector pAdEasy into *E. coli*. as described in (59).

fusion proteins of the expected size and cellular locations (**Figure 10**). Xdh/Xo, which is a soluble protein, remained in the supernatant when cell lysates were centrifuged. The molecular weight for Xdh/Xo monomer is 150 kDa and EYFP is 27 kDa. Therefore the theoretical molecular weight for fusion protein Xdh-EYFP is 177 kDa. The protein bands detected by Western Blot have an estimated size of about 170 kDa, which is very close to the expected size of 177 kDa. Btn1a1 is a membrane protein; it stays in the post-nuclear pellet after centrifugation of the cell lysates. The molecular weight of Btn1a1 is 67 kDa. Therefore the expected size for fusion protein Btn1a1-EYFP was determined to be 96 kDa by Western blot. The double bands of Btn1a1 (**Figure 10**, lanes 2, 3) are glycosylated variants, confirmed by digesting with N-glycanase to remove the N-linked glycan (Mather, I.H. unpublished observations).

After we had confirmed that the Btn1a1 and Xdh/Xo proteins were expressed as full-length proteins, the corresponding adenoviral vectors were also tested. Adenoviral vectors encoding Adv-BTN-EYFP or Adv-XDH-EYFP were added to HEK293 cells at vector /cell ratios ranging from 0.1 to 25 pfu/ cell. For Adv-BTN-EYFP, cells appeared to be healthy after culture overnight, except for cultures transduced with 25 pfu/ cell, which were detached and necrotic. Cells were healthy when treated with adenoviral vector titer below 10 pfu/ cell. Fluorescent fusion protein was observed in cells transduced with titers between 1-10 pfu/ cell for Adv-BTN-EYFP and 1 pfu/cell was considered optimal. Similar results were obtained for Adv-XDH-EYFP except that cells detached if more than 10 pfu/ cell of vectors were transduced. Cells were healthy when transduced with adenoviral vector titers at or

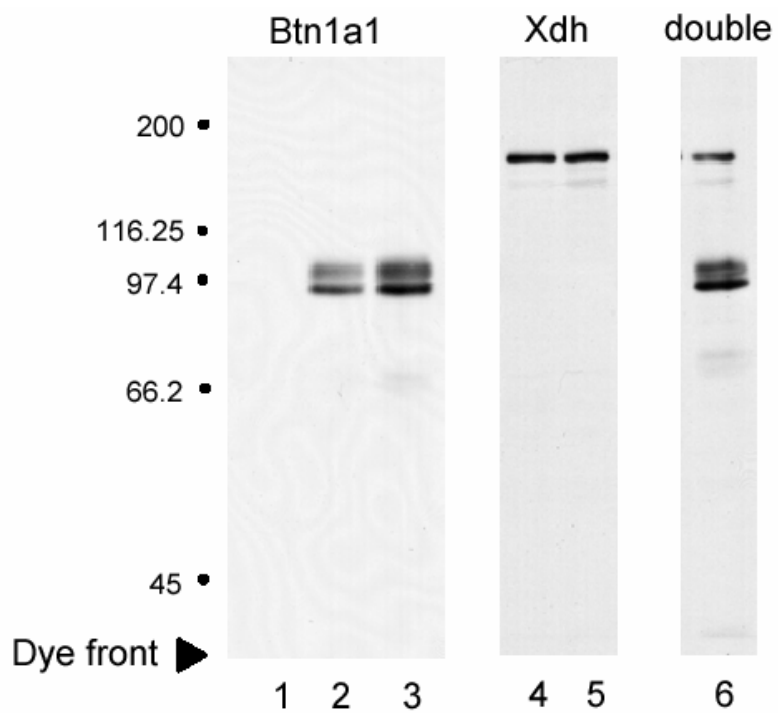


**Figure 10. Western blot of fusion proteins expressed in HEK293 cells**

Lanes 1, untransfected control; 2, Btn1a1-ECFP; 3, Btn1a1-EYFP; 4, Xdh-ECFP; 5, Xdh-EYFP; 6, Btn1a1-ECFP and Xdh-EYFP together.

below 1 pfu/ cell (**Figure 11, 12**).

To test whether fusion proteins of Btn1a1 or Xdh/Xo with EYFP were expressed as full-length proteins in cells transduced with the adenoviral vectors, the respective adenoviral vectors were added to HEK293 cells at the optimal vector/ cell ratios determined above. After overnight incubation, cells were lysed and separated into soluble and membrane fractions. Fractions were analyzed by SDS-PAGE and Western Blot using anti-GFP antibody (**Figure 13**). Proteins of the expected sizes, namely 170,000 for the fusion proteins of Xdh/Xo and 96,000 for Btn1a1, were detected in the post-nuclear supernatant and pellet fractions respectively. More protein was detected in cells transduced with higher titers of adenoviral vector.

Having shown that full-length fusion proteins of Btn1a1 and Xdh/Xo tagged with EYFP were expressed in HEK293 cells with the respective adenoviral vectors, the cellular distributions of the fusion proteins were determined by fluorescence microscopy. As expected, Btn1a1 was targeted to the plasma membrane, whereas Xdh/Xo, a soluble protein, was distributed throughout the cytoplasm (**Figure 14**). Btn1a1 was also present in intra-cellular organelles, most probably the rER and Golgi complex.

We next examined the expression of Btn1a1-EYFP and Xdh-EYEP in lactating mammary tissue. Lactation in the mouse increases after the second day post-partum, reaches a peak in the 10<sup>th</sup> day, and neonates are typically weaned at the 20<sup>th</sup> day of the lactation cycle. Due to development of alveoli in the mammary gland and the accumulation of secretory product, the infusion process was held as close to

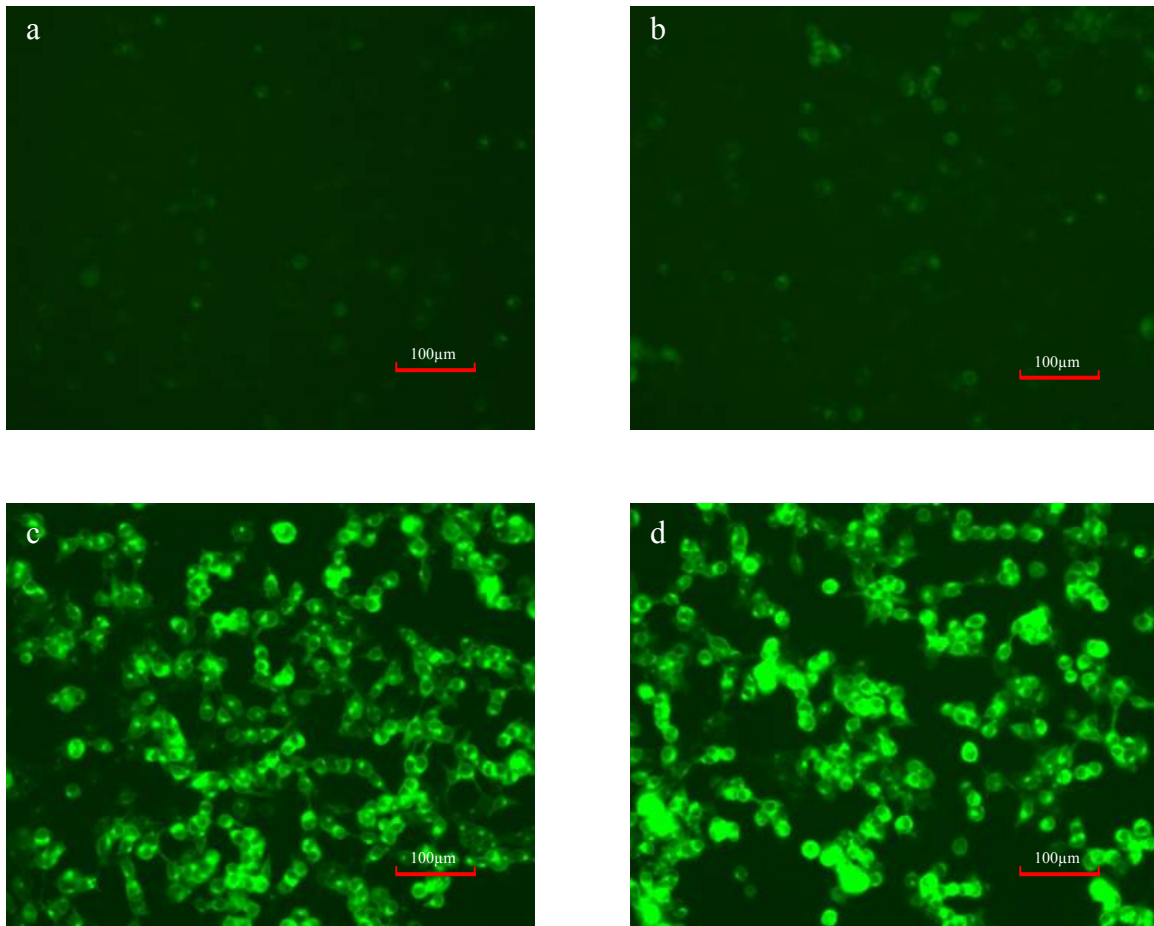


**Figure 11. Transduction of HEK293 cells with Adv-BTN-EYFP adenoviral vector**

Cells were incubated overnight at 37°C, in 5% CO<sub>2</sub> 95% air, divided equally, and grown to 60 to 80% confluency before transduction. Cells were examined after 16 h by fluorescence microscopy. Cells in all plates but those treated with 25 pfu/ cell grew well. Fluorescence signals were parallel to the transduction titer. (a) 0.1 pfu/ cell; (b) 1 pfu/ cell; (c) 10 pfu/ cell; (d) 25 pfu/ cell. Bar, 100 μm.

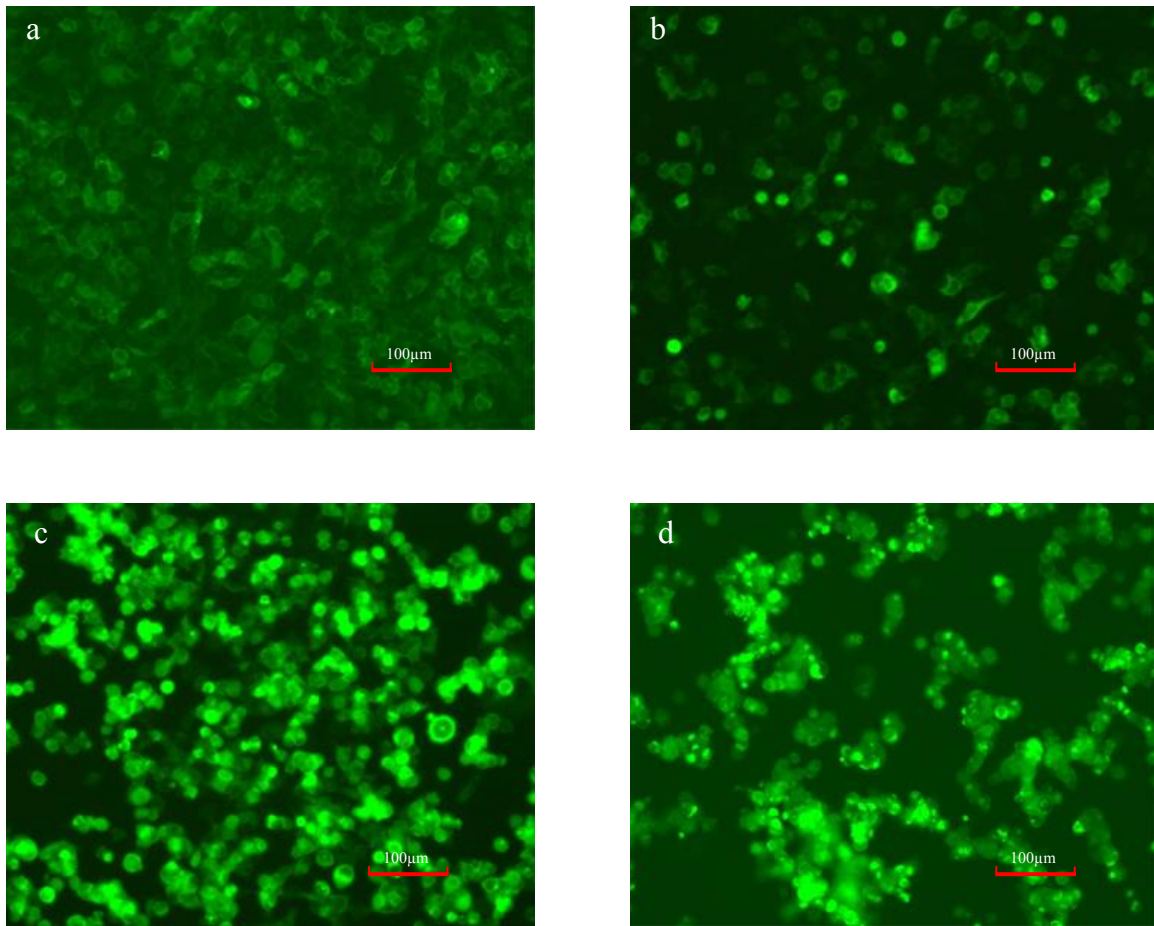


**Figure 12. Transduction of HEK293 cells with Adv-XDH-EYFP adenoviral vector**

Experimental conditions were as described in the legend to Figure 11. (a) 0.1 pfu/ cell; (b) 0.4 pfu/ cell; (c) 1 pfu/ cell; (d) 10 pfu/ cell. Bar 100  $\mu\text{m}$ .

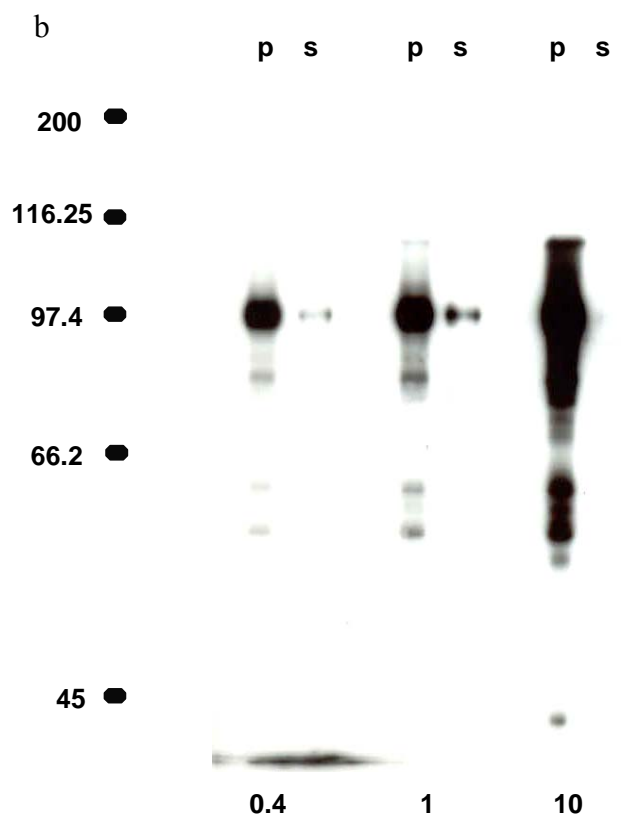
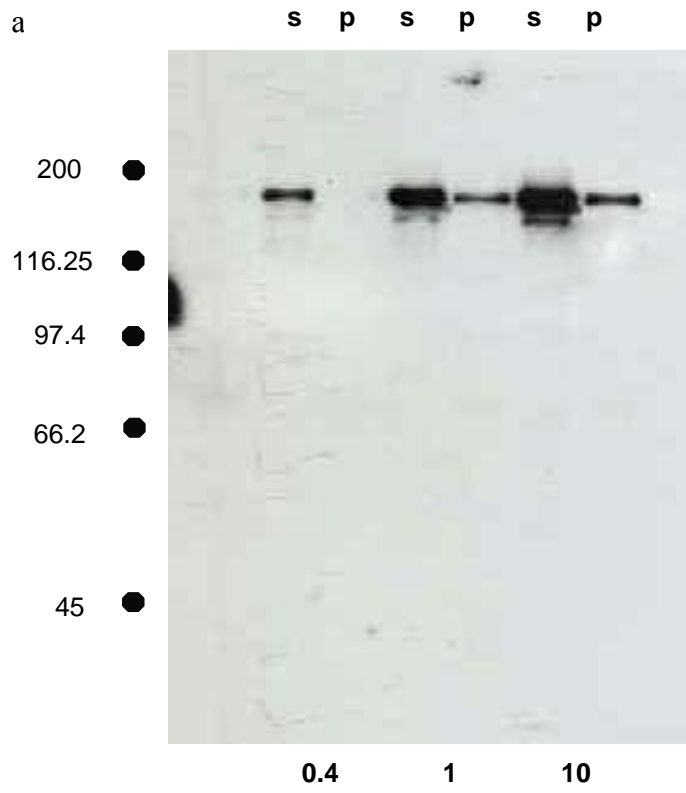


**Figure 13. Expressed fusion proteins of Xdh/Xo and Btn1a1 with EYFP in HEK293 cells, transduced with Adv-XDH-EYFP or Adv-BTN-EYFP**

Cells transduced with Adv-BTN-EYFP or Adv-XDH-EYFP, respectively, were lysed in lysis buffer, and fractionated by centrifugation at 15,000  $g_{av}$  for 30 min at 4°C. Samples (20  $\mu$ g protein/ lane) were separated by SDS-PAGE and analyzed by Western Blot, using anti-GFP antibody. (a) HEK293 cells transduced with Adv-XDH-EYFP at titers of 0.4, 1, and 10 pfu/ cell, respectively as indicated. The fusion protein was mostly detected in the post-nuclear supernatant. (b) HEK293 cells transduced with Adv-BTN-EYFP at titers of 0.4, 1, and 10 pfu/ cell, respectively as indicated. The fusion protein was mostly detected in the pellet.

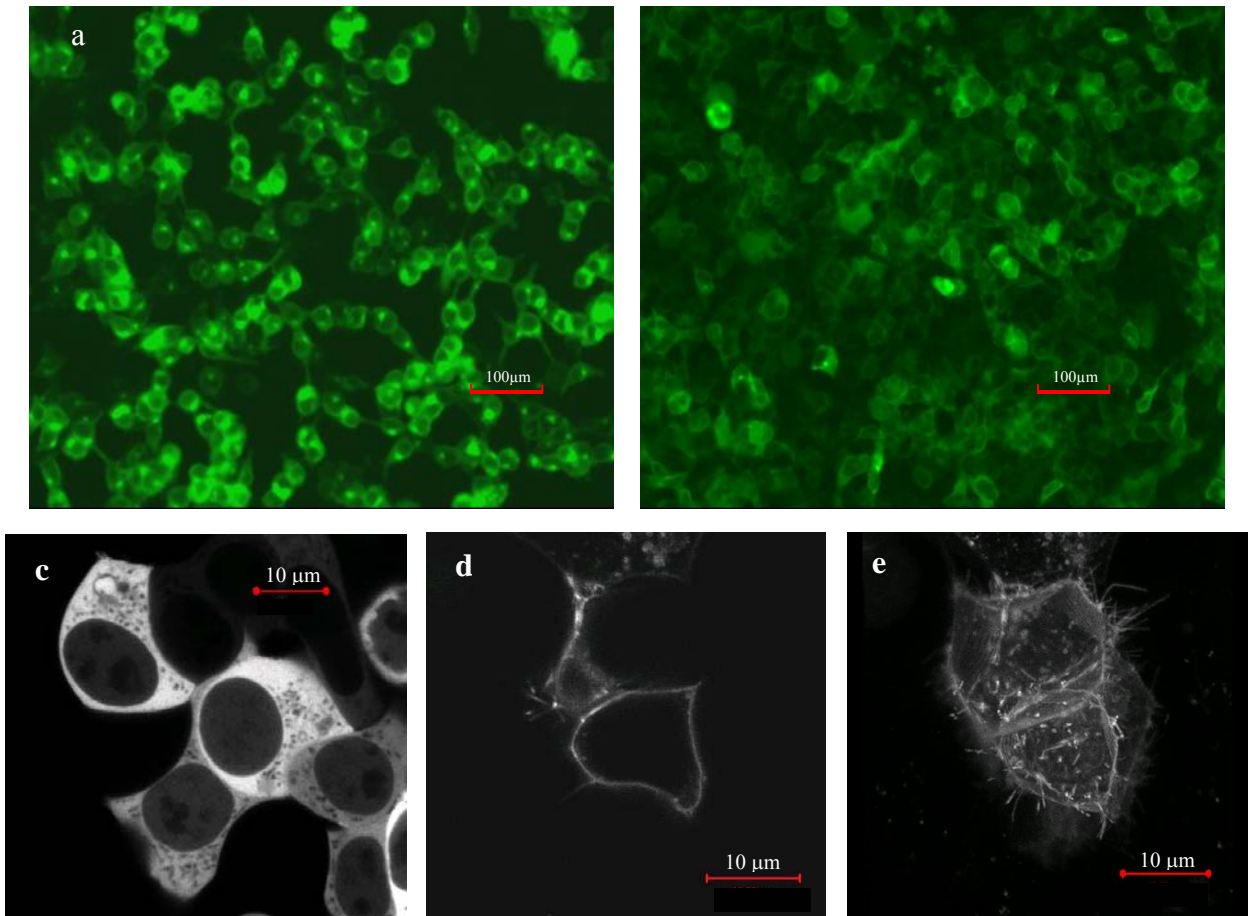


**Figure 14. Distribution of fusion proteins Btn-EYFP and Xdh-EYFP in HEK293 cells**

Cells were transduced with either 1 pfu/ cell of Adv-BTN-EYFP in (a), or 0.1 pfu/ cell of Adv-XDH-EYFP in (b). Experimental conditions were as described in Figure. 12. Bar 100  $\mu\text{m}$ . Distribution of Xdh-EYFP and Btn-EYFP in HEK293 cells studied by confocal microscopy, (c) Xdh-EYFP; (d, e) Btn-EYFP. Bar 10  $\mu\text{m}$ .

parturition as possible. To estimate the optimum developmental time for expression of fusion proteins, transduced glands were milked at different stages of lactation and the presence of fluorescent fusion proteins in the milk-lipid droplets were examined by microscopy.

The fourth mammary glands of C57/BL6 mice were infused with Adv-BTN-EYFP and Adv-XDH-EYFP adenoviral vectors with  $2.7 \times 10^7$  pfu vector/ gland on the 17<sup>th</sup>, 18<sup>th</sup>, and 19<sup>th</sup> days of pregnancy and milk was collected on the 3<sup>rd</sup>, 6<sup>th</sup>, 12<sup>th</sup>, 15<sup>th</sup>, and 17<sup>th</sup> days of lactation. Day 3 of lactation was the earliest practical time that milk could be collected. On the 3<sup>rd</sup> day of lactation about 20 percent of the milk-lipid droplets were labeled with fluorescent fusion protein (**Figure 15, 16**). The ratio of fluorescently-labeled lipid droplets decreased to approximately 10 percent on the 6<sup>th</sup> day. After the 6<sup>th</sup> day, the ratio dropped drastically until the end of lactation, at which time there was a minimal amount of protein expression. Mice were killed either on the day before or right after weaning (19<sup>th</sup>, or 20<sup>th</sup> day of lactation). Fluorescence microscopy of the whole mammary gland showed some parts, especially the nipple area, were still expressing fusion proteins at this time (data not shown). The same experiment was replicated in two other C57/ BL6 mice with similar results (data not shown). Mice infused during early lactation did not express fusion protein. Based on these results, we conclude that the optimal developmental period for expression of fusion proteins is between days 3-6 of lactation, with day 3 (the earliest collecting practicable time) being preferable.

We next used these optimal conditions for the transduction of the mammary epithelium *in vivo*, to examine the distribution of Btn1a1 and Xdh/Xo in lactating

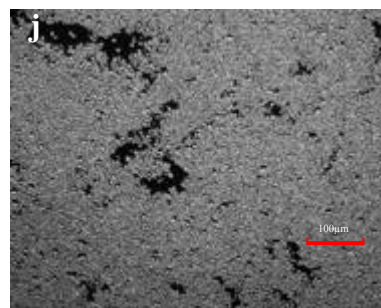
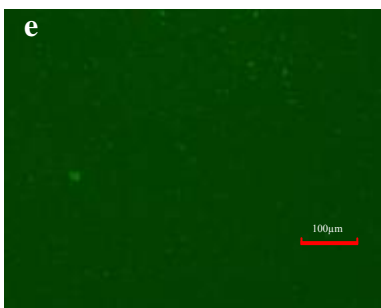
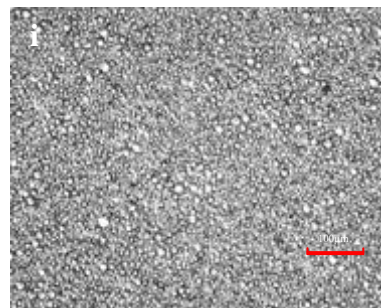
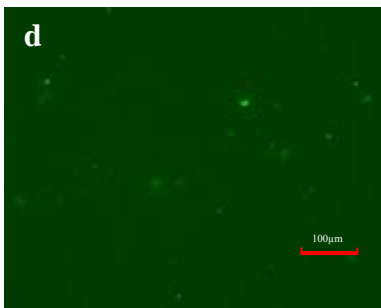
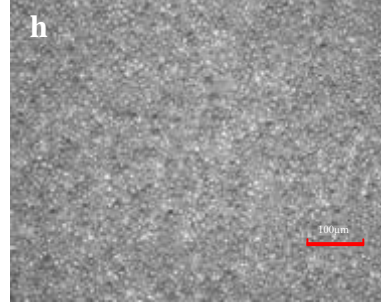
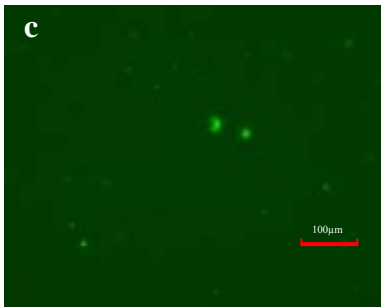
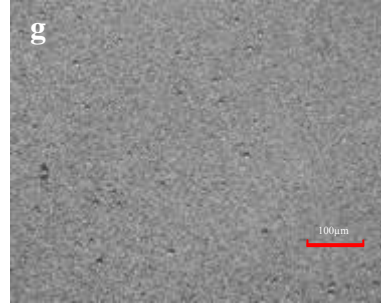
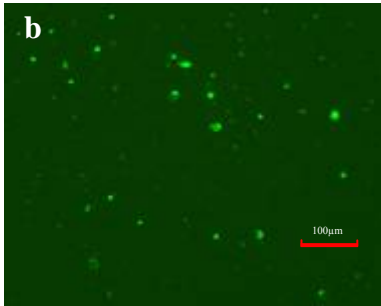
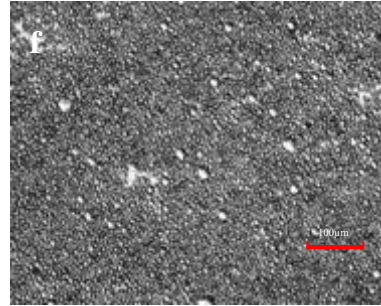
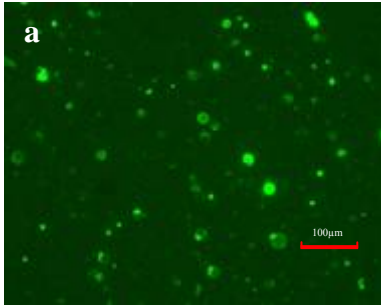


**Figure 15. Fluorescence microscopy of milk-lipid droplets from mouse mammary gland transduced with Adv-XDH-EYFP**

C57/BL6 mouse (infused in left fourth gland) was transduced with Adv-XDH-EYFP on the 19<sup>th</sup> day of pregnancy. Milk from the transduced gland was diluted with PBS in a volume ratio of 1 to 1, and examined by fluorescence and phase contrast microscopy. (a)- (e), fluorescence microscopy. (f)- (j), corresponding phase contrast micrographs. (a, f), day 3; (b, g), day 6; (c, h), day 12; (d, i), day 15; (e, j), day 17 of lactation. On day 3 and day 6 of lactation, 100 lipid droplets were counted in 3 randomly chosen areas, an average of 18 lipid droplets on day 3 and an average of 8 lipid droplets on day 6 were fluorescent (n=3). Bar 100  $\mu$ m.

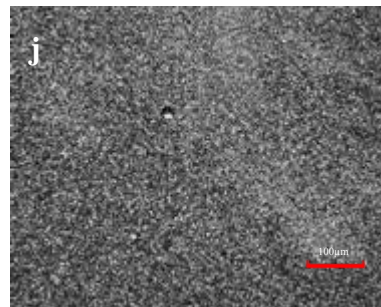
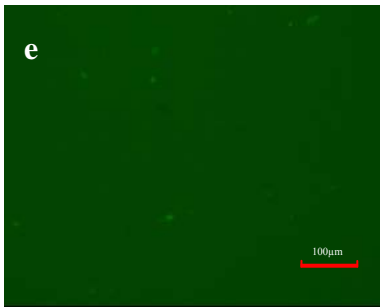
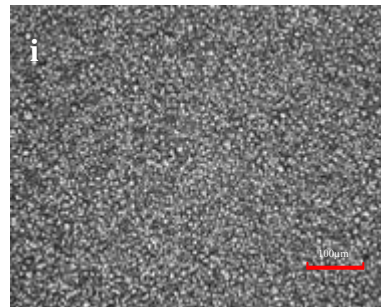
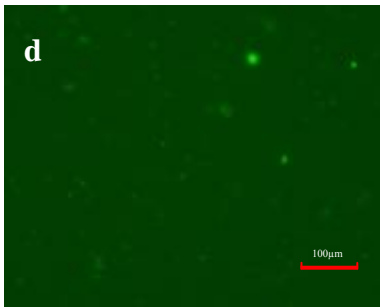
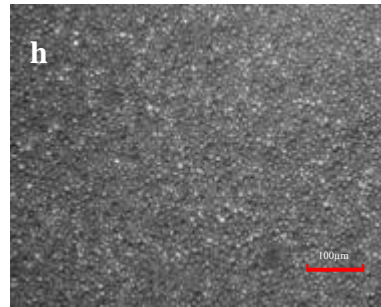
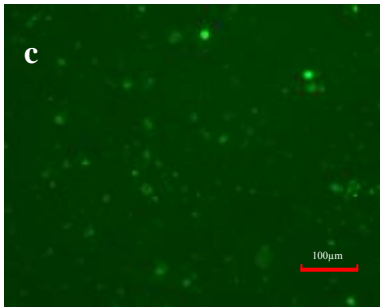
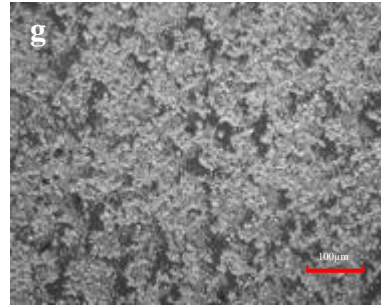
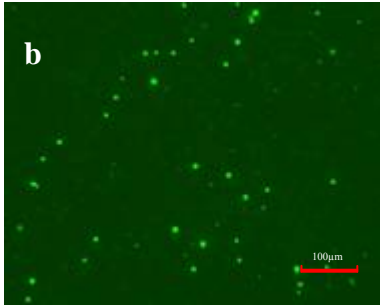
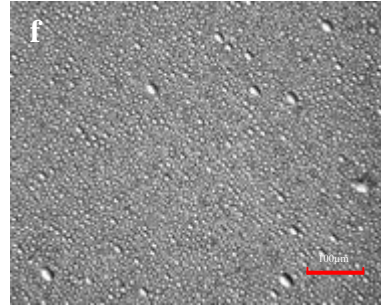
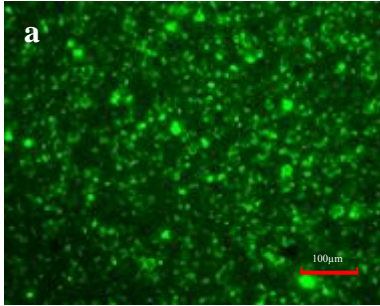


**Figure 16. Fluorescence microscopy of milk-lipid droplets from mouse mammary gland transduced with Adv-BTN-EYFP.**

C57/BL6 mouse (infused in right fourth gland) was transduced with Adv-BTN-EYFP on the 19<sup>th</sup> day of pregnancy. Milk from the transduced gland was diluted with PBS in a volume ratio of 1 to 1, and examined by fluorescence and phase contrast microscopy. (a)- (e), fluorescence microscopy. (f)- (j), corresponding phase contrast micrographs. (a, f), day 3; (b, g), day 6; (c, h), day 12; (d, i), day 15; (e, j), day 17 of lactation. On day 3 and day 6 of lactation, 100 lipid droplets were counted in 3 randomly chosen areas, an average of 21 lipid droplets on day 3 and an average of 10 lipid droplets on day 6 were fluorescent (n=3). Bar 100  $\mu$ m.

mammary gland and milk. A total of 23 mice were infused with adenoviral vectors Adv-BTN-EYFP or Adv-XDH-EYFP at different stages of pregnancy and early lactation (**Table 1**). Protein expression was highest in mice infused in as late a stage of pregnancy as possible and analyzed on the 3<sup>rd</sup> day of lactation. Approximately 30 percent of the transduced glands were fluorescent on that day. The extent of transduction was especially high in the nipple area and some parts of the distal area. Glands were transduced with either vector at the same level of efficiency (**Figure 17, 18**).

To test that full-length fusion proteins were expressed in the mouse mammary glands, two mice were infused with both adenoviral vectors on the 16<sup>th</sup> and 18<sup>th</sup> day of pregnancy and were killed on the 3<sup>rd</sup> day of lactation. Adv-BTN-EYFP or Adv-XDH-EYFP ( $2.7 \times 10^7$  pfu) was infused into the right and left 4<sup>th</sup> glands, respectively. Western blot analysis of the tissue fractions showed that both fusion proteins were expressed as full-length proteins (**Figure 19**; compare with **Figure 10, 13**).

To determine the distribution of Btn1a1 and Xdh/Xo in the mammary gland, we infused mouse mammary glands with either adenoviral vector in titers of either  $2 \times 10^7$  pfu into the 3<sup>rd</sup> gland or  $6 \times 10^7$  pfu into the 4<sup>th</sup> gland and examined frozen sections (6-8  $\mu\text{m}$ ) of tissue or milk samples by fluorescence microscopy.

For Adv-BTN-EYFP infused tissue, Btn1a1-EYFP was detected in the apical plasma membrane (**Figure 20**). For Adv-XDH-EYFP infused tissue, Xdh-EYFP was seen in the cytoplasm and surrounding lipid droplets (**Figure 21**). Btn-EYFP and Xdh-EYFP were also detected in secreted milk-lipid droplets. In both cases, the proteins were unevenly distributed around the droplet surface. Discontinuous

**Table 1: Summary of mice infused with adenoviral vector**

| Adenoviral Vector | Gland Infused       | Infusion day (pregnancy) | Sacrificed day (lactation) | Protocol   |
|-------------------|---------------------|--------------------------|----------------------------|--|
| Adv-BTN-EYFP      | 4 <sup>th</sup> , R | 17                       | 20                         | Milk collected in the 3 <sup>rd</sup> , 6 <sup>th</sup> , 12 <sup>th</sup> , 15 <sup>th</sup> , and 17 <sup>th</sup> day of lactation. |
| Adv-XDH-EYFP      | 4 <sup>th</sup> , L | 18                       | 21                         |  |
|                   |                     | 19                       | 20                         |  |
| Adv-XDH-EYFP      | 3 <sup>rd</sup> , L | 12                       | 3                          | Adv-XDH-EYFP infused tissue was fixed and studied by fluorescence microscopy.  |
| 3X Adv-XDH-EYFP   | 4 <sup>th</sup> , R | 16                       | 3                          |  |
|                   |                     | 17                       | 3                          |  |
|                   |                     | 18                       | 3                          |  |
|                   |                     | 19                       | 3                          |  |
| Adv-BTN-EYFP      | 4 <sup>th</sup> , R | 15                       | 3                          | Adv-BTN-EYFP infused tissue was fixed and studied by fluorescence microscopy.  |
| 3X Adv-BTN-EYFP   | 3 <sup>rd</sup> , R | 16                       | 3                          |  |
|                   |                     | 17                       | 3                          |  |
|                   |                     | 17                       | 3                          |  |
|                   |                     | 19                       | 3                          |  |
| Adv-BTN-EYFP      | 4 <sup>th</sup> , R | 16                       | 3                          | Infused tissue was analyzed by Western blot.   |
| Adv-XDH-EYFP      | 4 <sup>th</sup> , L | 18                       | 3                          |  |
| Adv-BTN-EYFP      | 4 <sup>th</sup> , R | 15                       | 3                          | Milk samples were studied by conventional fluorescence microscopy.   |
| Adv-XDH-EYFP      | 4 <sup>th</sup> , L | 16                       | 3                          |  |
|                   |                     | 18                       | 3                          |  |
|                   |                     | 19                       | 3                          |  |
| Adv-XDH-EYFP      | 4 <sup>th</sup> , L | 17                       | 3                          | Milk samples were studied by confocal fluorescence microscopy.   |
|                   |                     | 18                       | 3                          |  |
| Adv-BTN-EYFP      | 4 <sup>th</sup> , R | 18                       | 3                          | Milk samples were studied by confocal fluorescence microscopy.   |
|                   |                     | 19                       | 3                          |  |

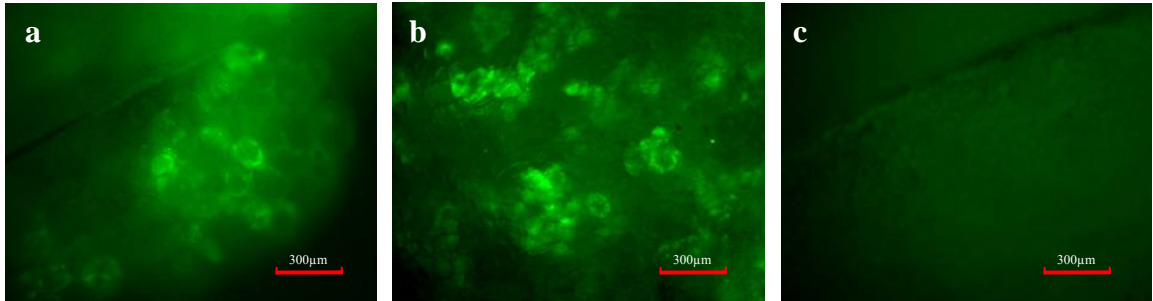


**Figure 17. Expression of Xdh-EYFP in whole mouse mammary gland transduced with Adv-XDH-EYFP**

A C57/ BL6 mouse was infused with Adv-XDH-EYFP on day 17 of pregnancy and sacrificed on day 3 of lactation. The infused and control glands were spread on microscope slides and fixed with 4% paraformaldehyde/ PBS at 4°C overnight. (a), nipple area; (b), distal area; (c), uninfused control gland. Bar 300 μm.

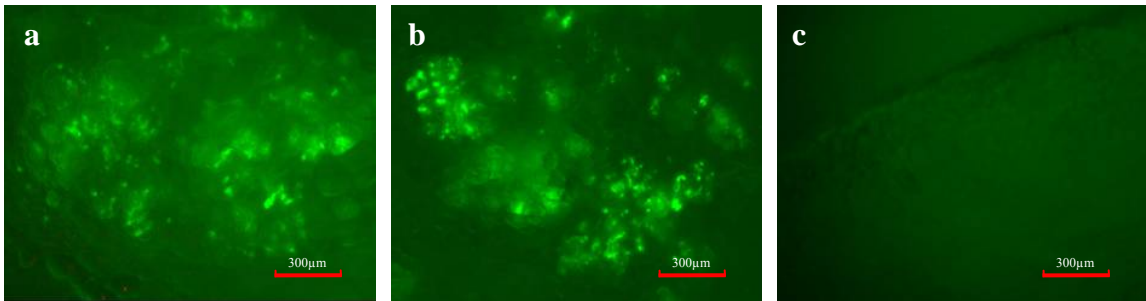


**Figure 18. Expression of Btn-EYFP in whole mouse mammary gland transduced with Adv-BTN-EYFP**

A C57/ BL6 mouse was infused with Adv-BTN-EYFP on day 19 of pregnancy and sacrificed on day 3 of lactation. The experimental conditions were as described in Figure 17. (a), nipple area; (b), distal area; (c), uninfused control gland. Bar 300  $\mu\text{m}$ .

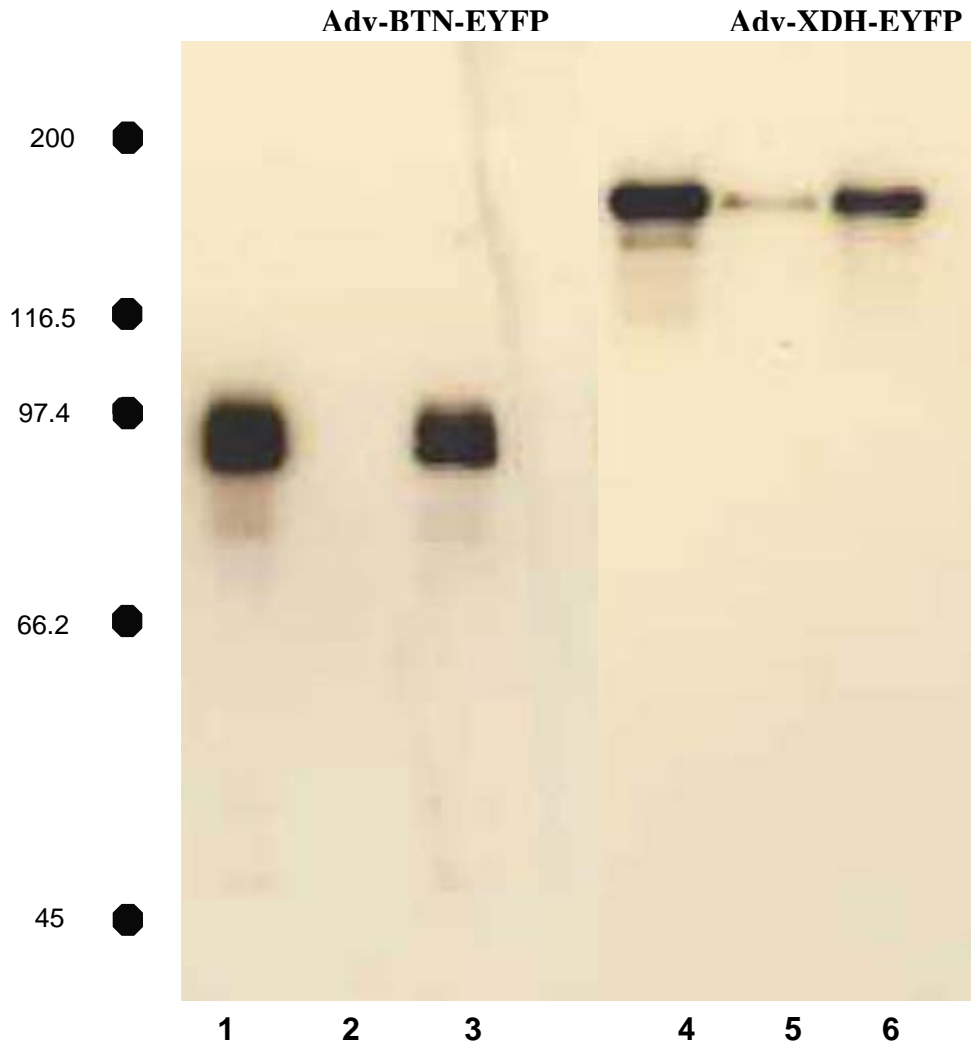


**Figure 19. Expression of Btn-EYFP and Xdh-EYFP in mouse mammary gland tissue transduced with either Adv-BTN-EYFP or Adv-XDH-EYFP.**

A C57/BL6 mouse was infused with Adv-BTN-EYFP or Adv-XDH-EYFP on the 16<sup>th</sup> day of lactation into right or left 4<sup>th</sup> gland, respectively, and sacrificed on the 3<sup>rd</sup> day of lactation. Milk was collected immediately before the mouse was killed. Mammary glands were homogenized in buffer containing protease inhibitors and fractionated into soluble and membrane fractions. Samples (20 µg protein/ lane) were separated by SDS-PAGE and analyzed by Western blot using anti-GFP antibody. Lanes 1, Adv-BTN-EYFP milk; 2, Adv-BTN-EYFP supernatant tissue fraction; 3, Adv-BTN-EYFP tissue pellet; 4, Adv-XDH-EYFP milk; 5, Adv-XDH-EYFP tissue pellet; 6, Adv-XDH-EYFP supernatant tissue fraction.

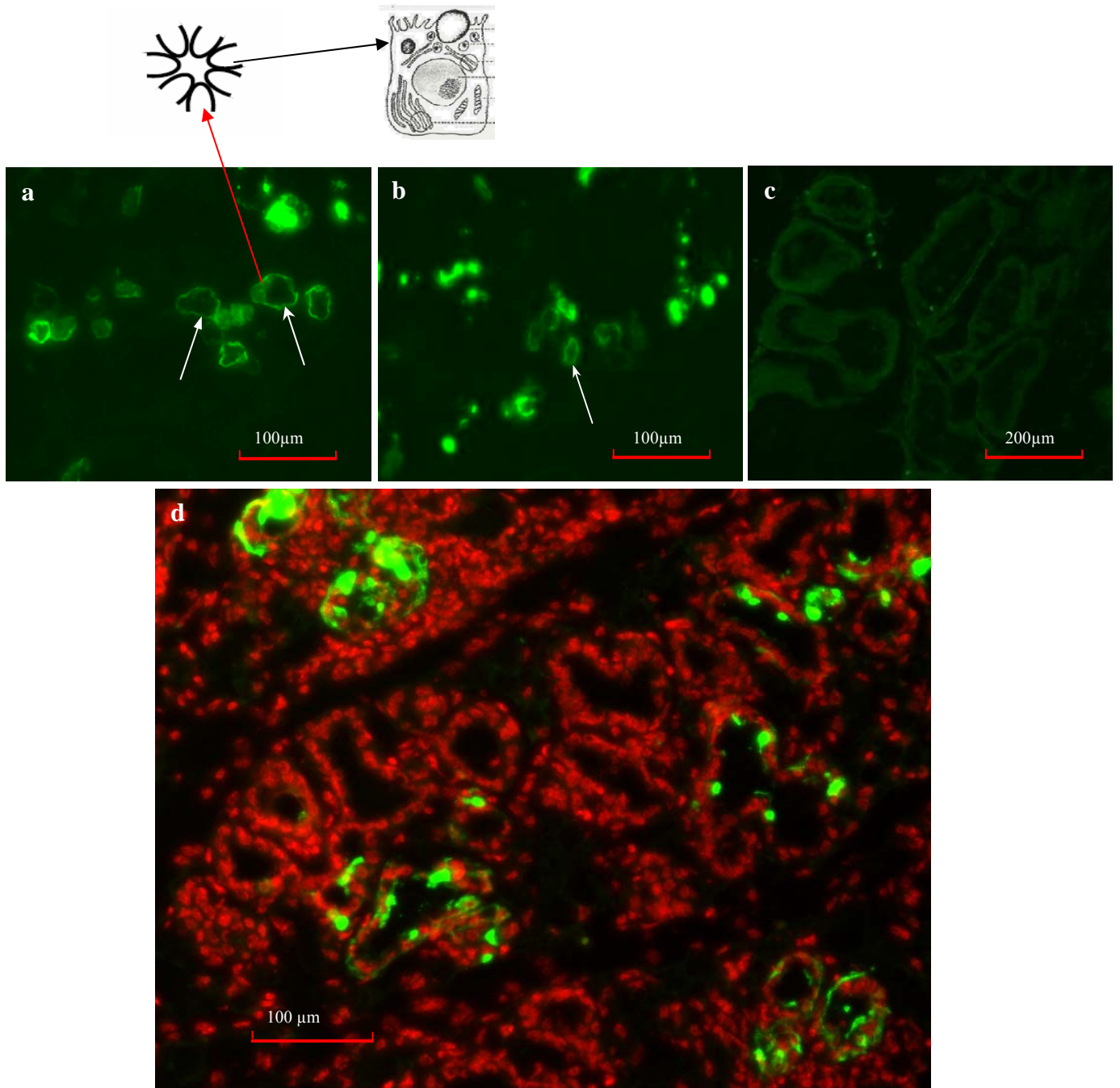


**Figure 20. Distribution of Btn-EYFP in mouse mammary gland transduced with Adv-BTN-EYFP.**

A C57/BL6 mouse was transduced with Adv-BTN-EYFP on day 17 of pregnancy and sacrificed on day 3 of lactation. Fixed/ frozen tissue was examined by fluorescence microscopy. Btn-EYFP is distributed in the apical plasma membrane of epithelial cells (arrows) (a), (b): tissue sections from gland; (c): uninfused control; (d,e): Adv-BTN-EYFP infused tissue sections stained with Dapi, bars, 100 µm.

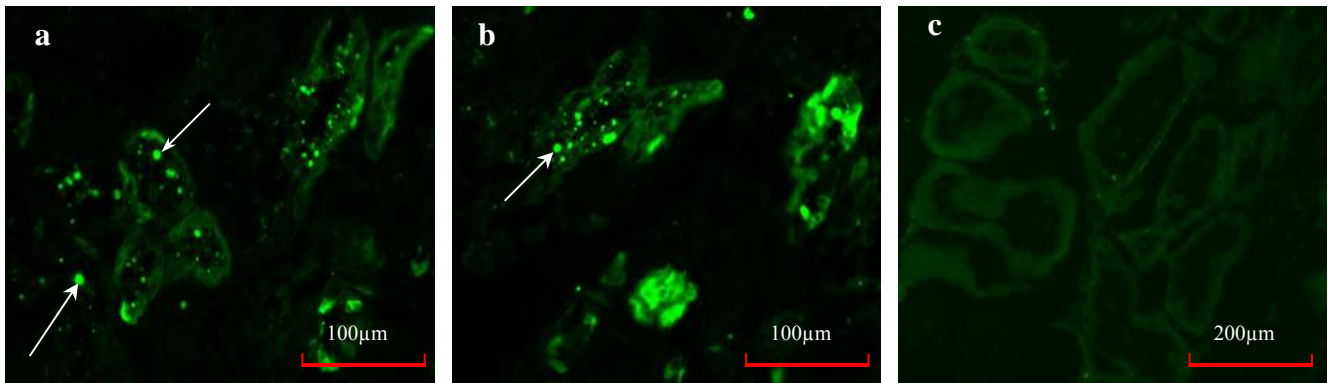


**Figure 21. Distribution of Xdh-EYFP in mouse mammary gland transduced with Adv-XDH-EYFP**

A C57/BL6 mouse was transduced with Adv-XDH-EYFP on day 18 of pregnancy and sacrificed on day 3 of lactation. Fixed/ frozen tissue was examined by fluorescence microscopy. Xdh-EYFP is distributed in the cytoplasm and presumptive lipid droplets in the cytoplasm and milk (arrows) (a), (b): tissue sections of infused gland; (c): uninfused control.

crescents and caps containing the fluorescent proteins were evident (**Figure 22, 23**). These results suggest that the membrane undergoes morphology changes after secretion. These results were confirmed by 3-D analysis of labeled lipid droplets by confocal microscopy (**Figure 24-27**).

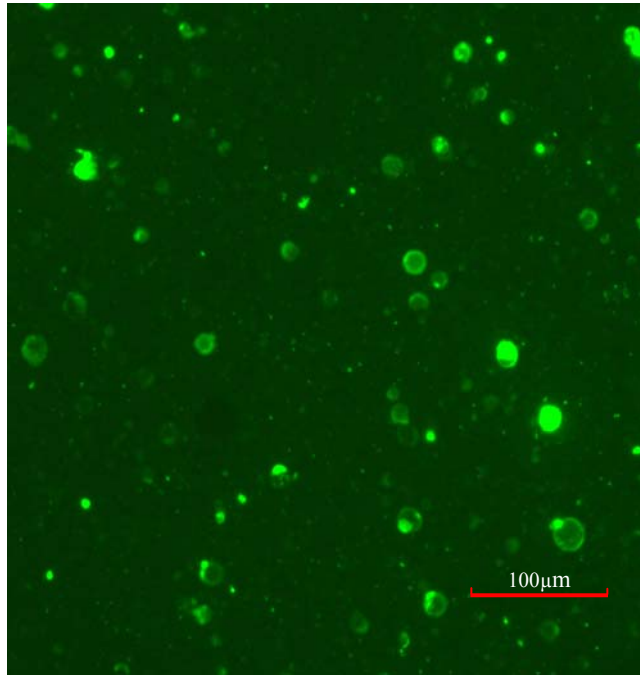


**Figure 22. Distribution of Btn-EYFP in secreted milk-lipid droplets**

A C57/BL6 mouse was infused with Adv-BTN-EYFP on day 15 of pregnancy. Milk was collected on the 3<sup>rd</sup> day of lactation and was studied by conventional fluorescence microscopy. Btn-EYFP was distributed unevenly, in the form of crescents, caps, and discontinuities, around many of the droplets, bars 100 μm.

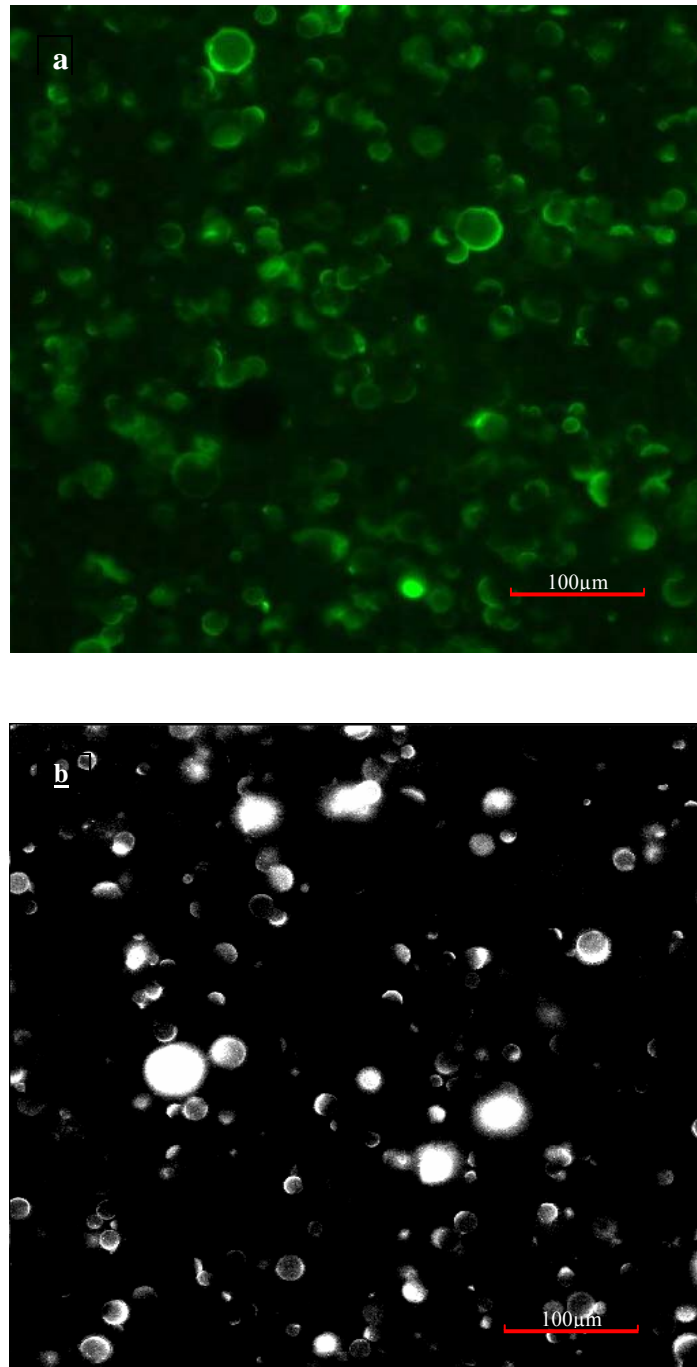


**Figure 23. Distribution of Xdh-EYFP in secreted milk-lipid droplets**

A C57/BL6 mouse was infused with Adv-XDH-EYFP on day 15 of pregnancy and milk was collected on the 3<sup>rd</sup> day of lactation. Xdh-EYFP was distributed unevenly, in the form of crescents, caps, and discontinuities, around many of the droplets. (a), conventional fluorescence micrograph; (b), confocal micrograph, bars 100 μm.

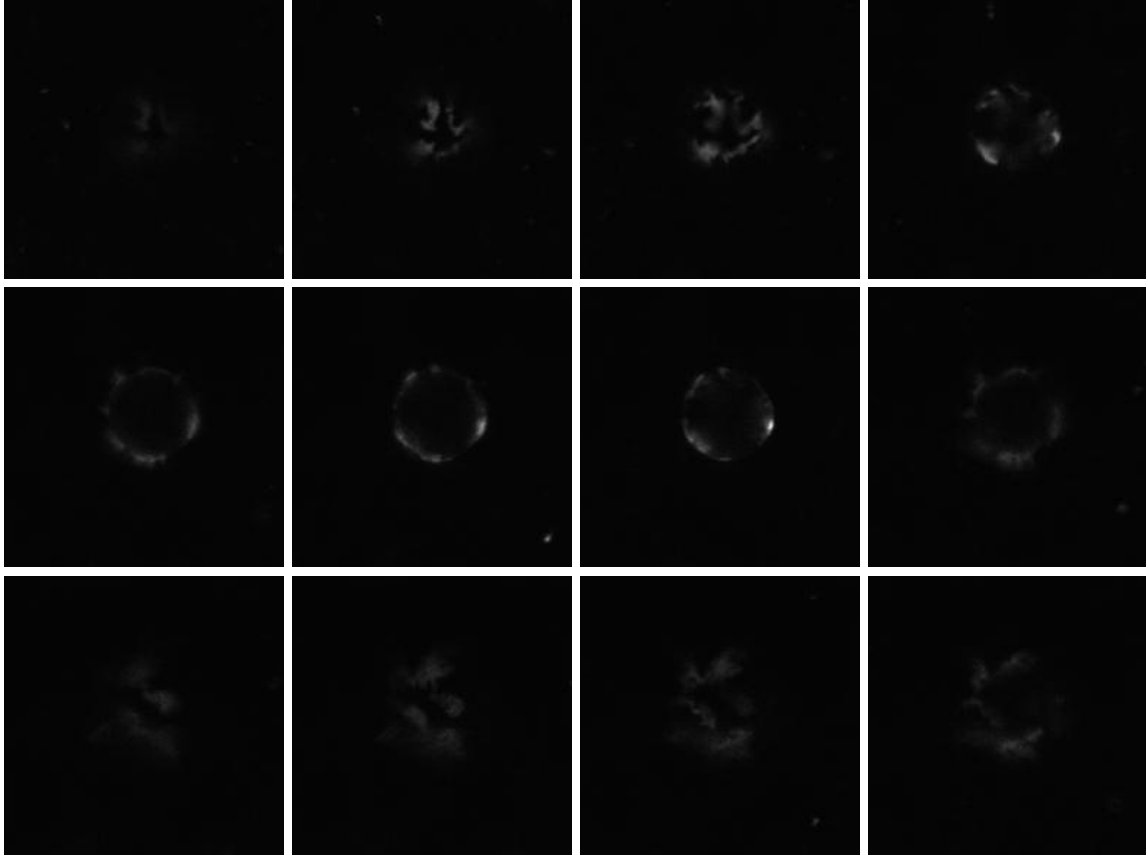


**Figure 24. Z-stack confocal micrographs of Xdh-EYFP labeled lipid droplet**

A C57/BL6 mouse was infused with Adv-XDH-EYFP on day 18 of pregnancy into the left 4<sup>th</sup> gland, and milk was collected on the 3<sup>rd</sup> day of lactation. Z-stack of 1  $\mu$ m confocal sections were taken. Note distribution of Xdh-EYFP is discontinuous on surface of lipid droplet.

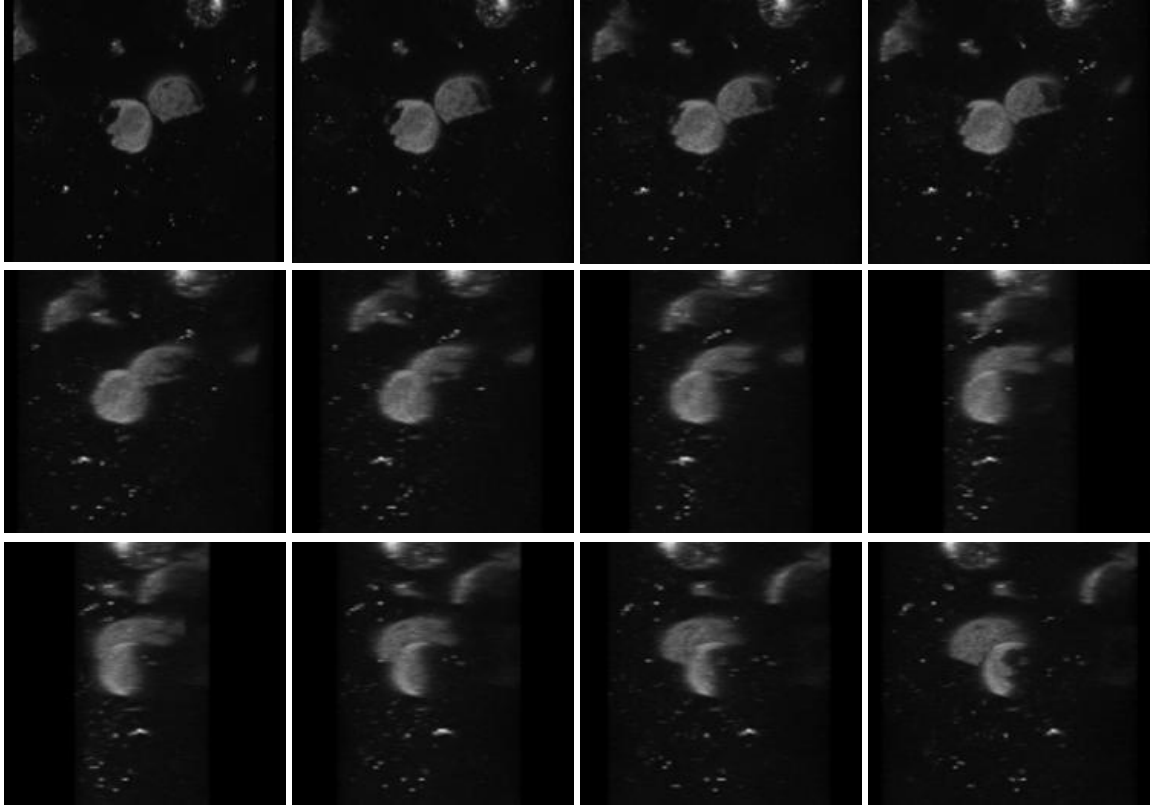


**Figure 25. 3-Dimensional reconstruction of Xdh-EYFP labeled lipid droplet**

Mouse infusion and milk collection were as described in the legend to Figure 24. The Xdh-EYFP is distributed in a cap, covering almost half of the lipid droplet.

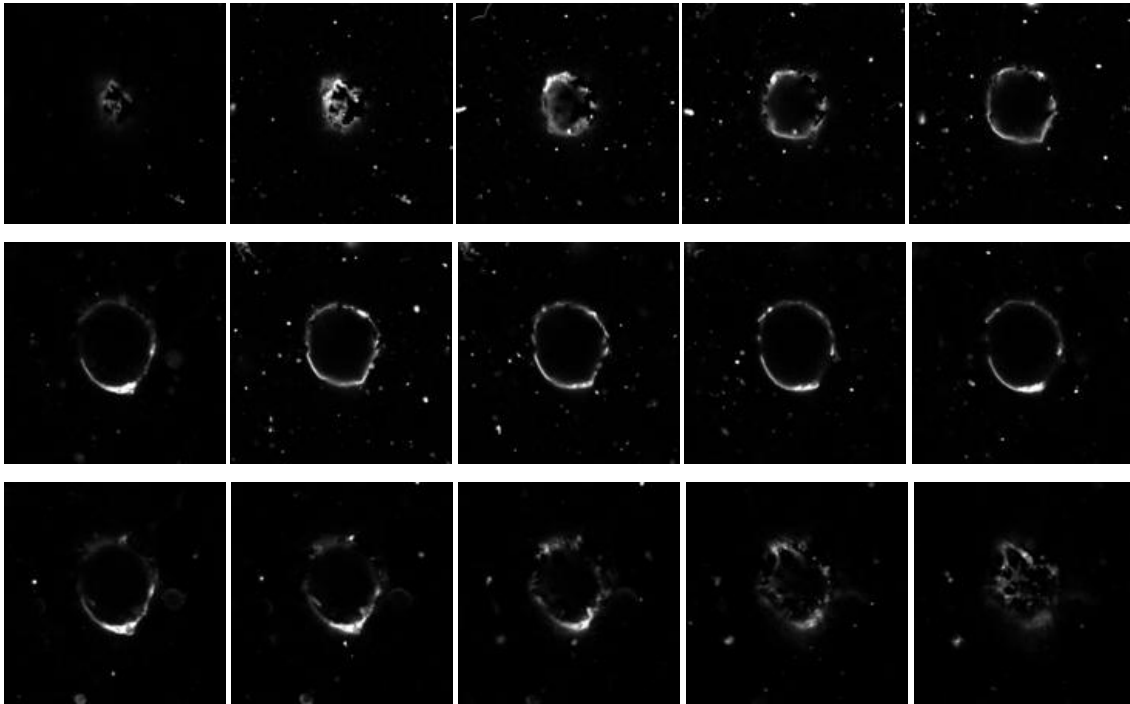


**Figure 26. Z-stack confocal micrographs of Btn-EYFP labeled lipid droplet**

A C57/BL6 mouse was infused with Adv-BTN-EYFP on day 18 of pregnancy to the right 4<sup>th</sup> gland, and milk was collected on the 3<sup>rd</sup> day of lactation. Z-stack of 1  $\mu$ m confocal sections were taken. Note distribution of Btn-EYFP is discontinuous on surface of lipid droplets.

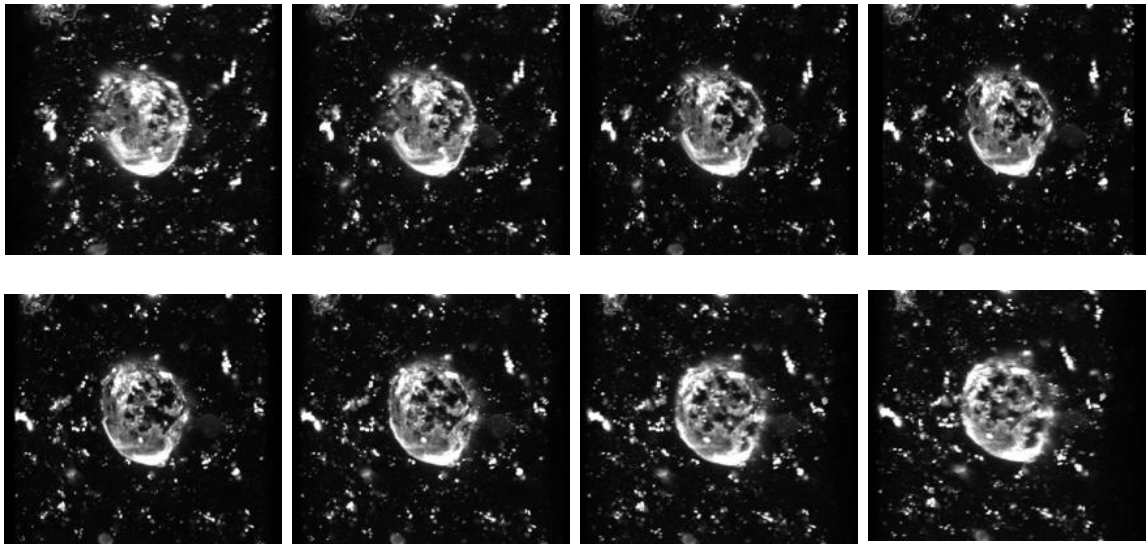


**Figure 27. 3-Dimensional reconstruction of Btn-EYFP labeled lipid droplet**

Mouse infusion and milk collection were as described in the legend to Figure 24. The Btn-EYFP is unevenly distributed on the surface of the lipid droplet.

## Discussion

Adenoviral-vector transduction has proven to be a suitable method for the efficient transduction of primary mammary cells, and *in vivo* transduction of mouse mammary glands has been evaluated for its efficacy and the potential problems of inflammation caused by the infused viruses and expressed proteins (53). This research has shown that infusion of adenoviral vectors in late pregnancy in the mouse leads to the successful transduction of the epithelial cells, which persists through the 5<sup>th</sup> day of lactation without causing localized inflammation (53).

Based on our experiments, we show that infusion of adenoviral vectors in late pregnancy is successful, and fusion protein expression is retained throughout lactation. Unlike the previous study of Russell *et al* (53), we did not encounter problems with tissue inflammation. The reason for this difference is not clear. Potential disadvantages of the adenoviral vector-infusion approach include problems in regulating the amount of protein expressed and potential instability of the expressed fusion proteins. However, we showed that both fusion proteins are stable in the transduced gland tissue (**Figure 19**). The potential overexpression of fusion proteins in the mammary gland needs to be addressed in future studies.

In this research, we determined the optimal time and persistence of protein expression by fluorescence microscopy. A total of 23 mice were transduced with either Adv-BTN-EYFPs or Adv-XDH-EYFPs (**Table 1**) and the optimal time of fusion protein expression was determined by fluorescence microscopy of freshly collected milk at different stages of lactation (**Figure 15, 16**). Day 3 of lactation is the

earliest time we could collect milk and a large amount of milk could be collected around day 10, sufficient milk was available for study until weaning. Three mice were infused, milked, sacrificed, and studied under the same conditions. Consistent results suggested that fusion proteins were optimally expressed during the early period of lactation, namely the 3<sup>rd</sup> to 6<sup>th</sup> day. This is consistent with the extent of mouse mammary gland development after lactation. Weak expression of fusion proteins persisted until the 20<sup>th</sup> day of lactation, at which time the litters were weaned and the animals were sacrificed. Two attempts to transduce the mouse mammary gland in early lactation (day 1 and 2 of lactation, data not shown) were unsuccessful possibly because of interference from accumulated milk products.

Determination of the optimum time for fusion protein expression was important because it provides evidence that successful *in vivo* transduction is consistent with the development and physiological status of the mammary gland due to pregnancy and lactation. In addition, it enables us to study the distribution of fusion proteins under optimal circumstances.

Investigations of Btn1a1 and Xdh/Xo suggest that these two proteins function in milk-lipid secretion. Btn1a1 and Xdh/Xo are the two most abundant proteins in bovine MLGM (8) and both proteins are increased in expression and activity during pregnancy and lactation (32, 41, 47, 61). Moreover, Btn1a1 knock-out mice and Xdh/Xo heterozygous mice display abnormalities and disorganization in milk-lipid secretion (33, 50).

Several studies based on molecular cloning techniques, topological assays, membrane fraction composition assays, and conventional immunomicroscopy have

been employed to determine the distribution of Btn1a1 and Xdh/Xo in lactating mammary tissue (29, 32, 42, 49). Investigators have suggested that Btn1a1 is concentrated at the apical membrane of secretory epithelial cells (9, 32, 61). However, questions about the results remain, partly because of several technical difficulties encountered when processing mammary tissue for microscopy. Most critically, for conventional immunomicroscopy, a balance has to be maintained between keeping the tissue in optimal morphology during preparation and fixation and in retaining the capability of antibodies to bind to epitopes within the tissue sections. This is especially difficult for lipid-rich tissues such as lactating mammary gland. By the approach of expressing adenoviral vectors encoding fusion proteins of Btn1a1 and Xdh/Xo with variants of GFP, we can eliminate fixation artifacts and directly examine frozen tissue sections, which are preserved without chemical damage.

To study the distribution of Btn1a1 and Xdh/Xo, we successfully transduced lactating mouse mammary tissue with adenoviral vectors encoding either protein fused to GFP variants. The approach of adenoviral vector-infusion into mouse mammary gland (53) provides new opportunities for examining the distribution of Btn1a1 and Xdh/Xo by fluorescence microscopy. A recent immune study employing Epon-embedded tissue sections and anti-peptide antibodies to Btn1a1 and Xdh/Xo showed clearly that Btn1a1 is localized to the apical membrane, and Xdh/Xo to the surface of intracellular lipid droplets (Wooding and Mather, unpublished data). The *in vivo* results presented in this thesis are consistent with this study in that Btn1a1 is located at the apical plasma membrane (**Figure 20**), and Xdh/Xo is distributed in the

cytoplasm and surrounding lipid droplets (**Figure 21**). Both Btn1a1 and Xdh/Xo are localized in secreted milk-lipid droplets (**Figure 15, 16**). Fusion proteins of either Btn1a1 or Xdh/Xo were expressed as full-length proteins and in the expected locations. Furthermore, milk-lipid synthesis and secretion were regulated and normal, suggesting that the addition of EYFP did not affect the function of Btn1a1 and Xdh/Xo.

Potential post-secretion changes in the structure of the MLGM have been debated for over 35 years (22, 28). Wooding originally proposed that the MLGM condenses the surface of the lipid droplet, vesiculates and blebbs off into skim milk (22). Thus the MLGM was postulated to consist of a continuous membrane immediately after the droplet's separation from the secretory cell but to then undergo substantial structural rearrangements, including blebbing and the formation of crescents, and vesicles after secretion (22, 23, 24, 26). However, this mechanism was not accepted by many investigators because the tissue sections were fixed with glutaraldehyde and treated with post-fixation osmic acid and dehydrated.

Freeze-etch study of membrane fusion during secretion (62) and of bovine MLGM (28) has supported Wooding's proposals and a schematic model was introduced that provided a temporal description of post secretion membrane rearrangements (28). However, direct visualization of these rearrangements *in vivo* was lacking until we were able to express fluorescently tagged fusion proteins in lactating mammary gland directly. As shown by confocal microscopy, the protein and membrane coat of milk-lipid droplets is not evenly distributed around the lipid droplet. Crescent-like-structures and blebbings in the middle of a continuous

membrane were observed, confirming Wooding's original interpretation of electron micrographs. Thus as we propose now, the inner membrane of MLGM and the outer surface of the milk-lipid droplet interact with each other and ultimately fuse, leading to thickened areas of protein coat under crescents and membrane vesicles.

Based on the adenoviral vector infusion project, many promising future directions are possible. FRAP and FLIP procedures can be initiated to determine the mobility of proteins in membranes before and after secretion and FRET can be used to investigate the binding and interaction between Btn1a1 and Xdh/Xo at the apical membrane *in vivo*.

## References

1. Oftedal, O.T. (2002). The mammary gland and its origin during synapsid evolution. *J. Mammary Gland Biol. Neoplasia* 3, 225-252.
2. Hollmann, K. H. (1974) Cytology and fine structure of the mammary gland. *In* Lactation: a Comprehensive Treatise, vol I, pp 3-95, publ. Academic Press, Inc., NY.
3. Wilde, C. J., Knight, C.H., and Flint, D.J. (1999) Control of milk secretion and apoptosis during mammary involution. *J. Mammary Gland Biol. Neoplasia*, 4: 129-136.
4. Messer, M., and Urashima, T. (2002). Evolution of milk oligosaccharides and lactose. *Trends Glycosci. Glycotech.* 14: 153-176.
5. Linzell, J.L., and Peaker, M. (1971) Mechanism of milk secretion. *Physiol. Rev.* 51: 564-597.
6. Mather, I.H., and Keenan, T.W. (1983). Function of endomembranes and the cell surface in the secretion of organic milk constituents. T. B. Mepham. 231–283. Amsterdam, Elsevier. *Biochemistry of Lactation*.
7. Welsch, U., Schumacher, U., Buchheim, W., Schinko, I., Jenness, P., and Patton, S. (1990). Histochemical and biochemical observations on milk-fat-globule membranes from several mammalian-species. *Acta Histochemica. Suppl.* 40: 59-64.
8. Mather, I. H. (2000). A review and proposed nomenclature for major proteins of the milk-fat globule membrane. *J. Dairy Sci.* 83:203–247.
9. Mather, I. H., and Keenan, T. W. (1998). Origin and secretion of milk-lipids. *J. Mammary Gland Biol. Neoplasia* 3, 259-273.

10. Patton, S., and Jensen, R.G. (1975). Lipid metabolism and membrane functions of the mammary gland. In R.T. Holman (ed.). Progress in the Chemistry of Fats and other Lipids (vol. XIV) Part 4, Pergamon Press, Oxford, pp. 163-277.
11. Keenan, T.W., and Patton, S., in Jensen, R. G. (ed). (1995). Handbook of Milk Composition, Academic Press, San Diego CA. pp 5-50.
12. Wooding, F.B.P. (1974). Milk fat globule membrane material in skim-milk. *J. Dairy Res.* 41:331-337.
13. Stein, O., and Stein, Y. (1967). Lipid synthesis, intracellular transport, and secretion. Electron microscopic study of the mouse lactating mammary gland. *J. Cell Biol.* 34: 251-263.
14. Zaczek, M., and Keenan, T.W. (1990). Morphological evidence for an endoplasmic-reticulum origin of milk-lipid globules obtained using lipid-selective staining procedures. *Protoplasma* 159: 179-182.
15. Deeney, J. T., Valivullah, H. M., Dapper, C. H., Dylewski, D. P., and Keenan, T. W. (1985). Microlipid droplets in milk secreting mammary epithelial cells: Evidence that they originate from endoplasmic reticulum and are precursors of milk-lipid globules. *Eur. J. Cell Biol.* 38: 16-26.
16. Heid, H.W., Schnolzer, M., and Keenan, T.W. (1996). Adipocyte differentiation-related protein is secreted into milk as a constituent of milk-lipid globule membrane. *Biochem. J.* 320: 1025-1030.
17. Dylewski, D. P., Dapper, C.H., Valivullah, H.M., Deeney, J.T., and Keenan, T.W. (1984). Morphological and biochemical characterization of possible intracellular precursors of milk-lipid globules. *Eur. J. Cell Biol.* 35: 99-111.

18. Guerin, M.A., and Loizzi, R.F. (1980). Tubulin content and assembly states in guinea-pig mammary-gland during pregnancy, lactation, and weaning. *Proc. Soc. Exp. Biol. Med.* 165: 50-54.
19. Keenan, T.W., Dylewski, D.P., Ghosal, D., and Keon, B.H. (1992). Milk-lipid globule precursor release from endoplasmic reticulum reconstituted in a cell-free system. *Eur. J. Cell Biol.* 57: 21-29.
20. Stemberger, B.H., Walsh, R.M., and Patton, S. (1984). Morphometric evaluation of lipid droplet associations with secretory vesicles, mitochondria and other components in the lactating cell. *Cell Tiss. Res.* 236: 471-475.
21. Huston, G.E., and Patton, S. (1990). Factors related to the formation of cytoplasmic crescents on milk fat globules. *J. Dairy Sci.* 73: 2061-2066.
22. Wooding, F.B.P. (1971). The mechanism of secretion of the milk fat globule. *J. Cell Sci.* 9: 805-821.
23. Wooding, F.B.P. (1973). Formation of the milk fat globule membrane without participation of the plasmalemma. *J. Cell Sci.* 13:221-235.
24. Wooding, F. B. P. (1971). The structure of the milk fat globule membrane. *J. Ultrastruct. Res.* 37: 388-400.
25. Buchheim, W. (1982). Paracrystalline arrays of milk fat globule membrane-associated proteins as revealed by freeze-fracture. *Naturwissenschaften.* 69: 505-507.
26. Wooding, F. B.P., and Kemp, P. (1975). Ultrastructure of the milk fat globule membrane with and without triglyceride. *Cell Tiss. Res.* 165: 113-127.
27. Freudenstein, C., Keenan, T. W., Eigel, W. N., Sasaki, M., Stadler, J., and Franke, W.W. (1979). Preparation and characterization of the inner coat material

associated with fat globule membranes from bovine and human milk. *Exp. Cell Res.* 118: 277–294.

28. Da Silva, P., Menezes, A.P., and Mather, I.H. (1980). Structure and dynamics of the bovine milk fat globule membrane viewed by freeze fracture. *Exp. Cell Res.* 125: 127-139.

29. Banghart, L. R., Chamberlain, C. W., Velarde, J., Korobko, I. V., Ogg, S. L., Jack, L. J. W., Vakharia, V. N., and Mather, I. H. (1998). Butyrophilin is expressed in mammary epithelial cells from a single-sized messenger RNA as a type I membrane glycoprotein. *J. Biol. Chem.* 273: 4171-4179.

30. Heid, H. W., Winter, S., Bruder, G., Keenan, T. W., and Jarasch, E.-D. (1983). Butyrophilin, an apical plasma membrane-associated glycoprotein characteristic of lactating mammary glands of diverse species. *Biochim. Biophys. Acta.* 728: 228-238.

31. Taylor, M. R., Peterson, J. A., Ceriani, R. L., and Couto, J. R. (1996). Cloning and sequence analysis of human butyrophilin reveals a potential receptor function. *Biochim. Biophys. Acta.* 1306: 1-4.

32. Franke, W. W., Heid, H. W., Grund, C., Winter, S., Freudenstein, C., Schmid, E., Jarasch, E.-D., and Keenan, T. W. (1981). Antibodies to the major insoluble milk fat globule membrane associated protein: specific location in apical regions of lactating epithelial cells. *J. Cell Biol.* 89:485–494.

33. Ogg, S.L., Weldon, A.K., Dobbie, L., Smith, A.J., and Mather, I.H. (2004). Expression of butyrophilin (Btn1a1) in lactating mammary gland is essential for the

regulated secretion of milk-lipid droplets. *Proc. Natl. Acad. Sci. U S A* 101: 10084-10089.

34. Ye, T.-Z., Gordon, C. T., Lai, Y.-H., Fujiwara, Y., Peters, L. L., Perkins, A. C., and Chui, D. H. K. (2000). Ermap, a gene coding for a novel erythroid specific adhesion/ receptor membrane protein. *Gene* 242: 337-345.

35. Ruddy, D. A., Kronmal, G. S., Lee, V. K., Mintier, G. A., Quintana, L., Domingo, R., Meyer, N. C., Irrinki, A., McClelland, E. E., Fullan, A., Mapa, F. A., Moore, T., Thomas, W., Loeb, D. B., Harmon, C., Tsuchihashi, Z., Wolff, R. K., Schatzman, R. C., and Feder, J. N. (1997). A 1.1-Mb transcript map of the hereditary hemochromatosis locus. *Genome Res.* 7: 441-456.

36. Tazi-Ahnini, R., Henry, J., Offer, C., Bouissou-Bouchouata, C., Mather, I. H., and Pontarotti, P. (1997). Cloning, localization and structure of new members of the butyrophilin gene family in the juxta-telomeric region of the major histocompatibility complex. *Immunogenetics.* 47: 55-63.

37. Rhodes, D.A., Stammers, M., Malcherek, G., Beck, S., and Trowsdale, J. (2001). The cluster of *BTN* genes in the extended major histocompatibility complex. *Genomics.* 71: 351-362.

38. Vernet, C., Boretto, J., Mattei, M.-G., Takahashi, M., Jack, L.J.W., Mather, I.H., Rouquier, S., and Pontarotti, P. (1993). Evolutionary study of multigenic families mapping close to the human MHC class I region. *J. Mol. Evol.* 37: 600-612.

39. Henry, J., Mather, I. H., McDermott, M. F., and Pontarotti, P. (1998). B30.2-like proteins: update and new insights into a rapidly expanding family of proteins. *Mol. Biol. Evol.* 15: 1696-1705.

40. Grutter, C., Briand, C., Capitani, G., Mittl, P. R., Papin, S., Tschopp, J., and Grutter, M. G. (2006). Structure of the PRYSPRY-domain: Implications for autoinflammatory diseases. *FEBS Lett* 580: 99-106.
41. Ishii, T., Aoki, N., Noda, A., Adachi, T., Nakamura, R. And Matsuda, T. (1995). Carboxyterminal cytoplasmic domain of mouse butyrophilin specifically associateds with a 150 kDa protein of mammary epithelial cells and milk fat globule membrane. *Biochim. Biophys. Acta.* 1245: 285-292.
42. Jarasch, E.-D., Grund, C., Bruder. G., Heid, H.W., Keenan, T.W., and Franke, W.W. (1981). Localization of xanthine oxidase in mammary-gland epithelium and capillary endothelium. *Cell.* 25: 67-82.
43. Mather, I.H., Sullivan, C.H., and Madara, P.J. (1982). Detection of xanthine oxidase and immunologically-related proteins in fractions from bovine mammary tissue and milk after electrophoresis in polyacrylamide gels containing sodium dodecyl sulphate. *Biochem. J.* 202: 317-323.
44. Massey, V., and Harris, C.M. (1997). Milk xanthine oxidoreductase: the first one hundred years. *Biochem. Soc. Trans.* 25:750-755.
45. Clare, D. A., B. A. Blakistone, H. E. Swaisgood, and H. R. Horton. (1981). Sulfhydryl oxidase-catalyzed conversion of xanthine dehydrogenase to xanthine oxidase. *Arch. Biochem. Biophys.* 211:44-47.
46. Enroth, C., Eger, B. T., Okamoto, K., Nishino, T., and Pai, E. F. (2000). Crystal structures of bovine milk xanthine dehydrogenase and xanthine oxidase: Structure-based mechanism of conversion. *Proc. Natl. Acad. Sci. U. S. A.* 97: 10723-10728.

47. Kurosaki, M., Zanotta, S., Li Calzi, M., Garattini, E., and Terao, M. (1996). Expression of xanthine oxidoreductase in mouse mammary epithelium during pregnancy and lactation: regulation of gene expression by glucocorticoids and prolactin. *Biochem. J.* 319: 801–810.
48. Bruder, G., Heid, H.W., Jarasch, E.-D, and Mather, I.H. (1983). Immunological identification and determination of xanthine oxidase in cells and tissues. *Differentiation* 23: 218–225.
49. McManaman, J. L., Palmer, C. A., Wright, R. M., and Neville, M. C. (2002). Functional regulation of xanthine oxidoreductase expression and localization in the mouse mammary gland: evidence of a role in lipid secretion. *J. Physiol.* 545: 567-579.
50. Vorbach, C., Scriven, A., and Capecchi, M. R. (2002). The housekeeping gene xanthine oxidoreductase is necessary for milk fat droplet enveloping and secretion: gene sharing in the lactating mammary gland. *Genes Develop.* 16: 3223-3235.
51. Linzell, J. L., and Peaker, M. (1971). The permeability of mammary ducts. *J. Physiol.* 216:701-716.
52. Hens, J. R., Amstutz, M. D., Schanbacher, F. L., and Mather, I. H. (2000). Introduction of the human growth hormone gene into the guinea pig mammary gland by in vivo transfection promotes sustained expression of human growth hormone in the milk throughout lactation. *Biochim. Biophys. Acta* 1523:161-171.
53. Russell, T. D., Fischer, A., Beeman, N. E., Freed, E. F., Neville, M. C., and Schaack, J. (2003). Transduction of the mammary epithelium with adenovirus vectors *in vivo*. *J. Virol.* 77: 5801-5809.

54. Teter, B. B., Sampugna, J., and Keeney, M. (1990). Milk fat depression in C57Bl/6J mice consuming partially hydrogenated fat. *J. Nutr.* 120: 818-824.
55. Smith, P.K., Krohn, R.I., Hermanson, G.T., Mallia, A.K., Gartner, F.H., Provenzano, M.D., Fujimoto, E.K., Goeke, N.M., Olson, B.J., and Klenk, D.C. (1985). Measurement of protein using bicinchoninic acid. *Anal. Biochem.* 150: 76-85.
56. Laemmli, U. K. (1970). Cleavage of structural proteins during the assembly of the head of bacteriophage T4. *Nature* 227: 680-685.
57. Towbin, H., Staehelin, T., and Gordon, J. (1979). Electrophoretic transfer of proteins from polyacrylamide gels to nitrocellulose sheets: procedure and some applications. *Proc. Natl. Acad. Sci. U S A.* 76: 4350-4354.
58. Snapp, E. L., Hegde, R. S., Francolini, M., Lombardo, F., Colombo, S., Pedrazzini, E., Borgese, N., and Lippincott-Schwartz, J. (2003). Formation of stacked ER cisternae by low affinity protein interactions. *J. Cell Biol.* 163: 257-269.
59. He, T.C., Zhou, S., Da Costa, L.T., Yu, J., Kinzler, K.W., and Vogelstein, B. (1997). A simplified system for generating recombinant adenoviruses. *Proc. Natl. Acad. Sci. U S A.* 95: 2509-2514.
60. Akers, R.M. (2002). Selection for milk production from a lactation biology viewpoint. *J. Dairy Sci.* 83(5):1151-1158.
61. Johnson, V.G., and Mather, I.H. (1985). Monoclonal antibodies prepared against PAS-I butyrophilin and GP-55 from guinea-pig milk-fat-globule membrane bind specifically to the apical pole of secretory-epithelial cells in lactating mammary tissue. *Exp. Cell Res.* 158: 144-158.

62. Da Silva, P., and Nogueira, M. L. (1977). Membrane fusion during secretion. A hypothesis based on electron microscope observation of *Phytophthora Palmivora* zoospores during encystment. *J Cell Biol.* 73: 161-181.